STUDY OF MINIMUM WEIGHT DESIGN OF A STIFFENED CYLINDRICAL SHELL USING FINITE ELEMENT METHOD

by

MADHUKAR VABLE

DEPARTMENT OF AERONAUTICAL ENGINEERING

INDIAN INSTITUTE OF TECHNOLOGY KANPUR

JULY, 1976

STUDY OF MINIMUM WEIGHT DESIGN OF A STIFFENED CYLINDRICAL SHELL USING FINITE ELEMENT METHOD

A Thesis Submitted
In Partial Fulfilment of the Requirements
for the Degree of
MASTER OF TECHNOLOGY

by

MADHUKAR VABLE

to the

DEPARTMENT OF AERONAUTICAL ENGINEERING
INDIAN INSTITUTE OF TECHNOLOGY KANPUR
JULY, 1976

CERTIFICATE

Certified that the thesis entitled "Study of Minimum Weight Design of a Stiffened Cylindrical Shell Using Finite Element Method" is a bonafide work done by Sri M. Vable under our supervision and has not been submitted elsewhere for a degree.

N.G.R. Iyengar

Dr. N.G.R. IYENGAR
Assistant Professor
Dept. of Aeronautical Engg.
Indian Institute of Technology
Kanpur

Dr. S.S. RAO
Assistant Professor
Dept. of Mechanical Engg.
Indian Institute of Technology
Kanpur

ACKNOWLEDGEMENT

I wish to thank -

- Dr. S.S. Rao for his guidance and encouragement

- Dr. N.G.R. Iyengar for his valuable suggestions

- Ministry of Defence for sponsoring the project.

M. Vable

CONTENTS

Chapter			Page
	LIST OF TABLES		
	LIST OF FIGURES		
	LIST OF SYMBOLS		
	ABSTRACT		
1.	INTRODUCTION		1
2.	FORMULATION AND SOLUTION OF THE PROBLEM		6
	2.1	Formulation	6
	2.2	Interior Penalty Method of Solution	7
	2.2.1	Davidon-Fletcher-Powell Method	11
	2.2.2	One Dimensional Mini isation	13
3.	ANALYSIS OF THE STRUCTURE		15
	3.1	Doubly Curved Triangle	17
	3.1.1	Stiffness Matrix	17
	3.1.2	Consistant Load Vector	22
	3.1.3	Mass Matrix	24
	3.2	Constant Stress Triangle	25
	3.2.1	Stiffness Matrix	25
	3.2.2	Mass Matrix	28
	3.3	Evaluation of Constraints	29
	3.4	Subspace Iterative Scheme	30
	3.5	Comparative Study	32
	3.6	Conversion Study of C.S.T.	34

Chapter			Page
4.	RESULTS AND DISCUSSION		36
	4.1	Displacement and Frequency Gradients	36
	4.2	Cylindrical Shell Problem	38
	4.2.1	Parametric Study	39
	4.2.2	Minimum Weight Design	42
5.	CONCLUSIONS AND RECOMMENDATIONS		44
	5.1	Conclusions	44
	5.2	Recommendations	44
	REFERENCES		76
	APPENDIX A		79
	APPENDIX B		86

LIST OF TABLES

Table 1. Comparative study

Table 2. Convergence study

2.1 Variation of (EtV/p_oRL) along edge AB

2.2 Variation of $(EtW/p_oR^2\theta)$ along edge BC

2.3 Variation of ω_1 and ω_2

Table 3. Parametric study

Table 4. Optimisation results

LIST OF FIGURES

1. Schematic diagram of cubic interpolation
2. Finite element idealisation of the cylinder
3. Doubly curved triangle
4. Constant stress triangle
5. Spherical cap
7. Variation of (EtV/p_oRL) along edge AB
8 Variation of (EtW/p_oR^2) along edge BC
9. C.S.T. idealisations of a spherical cap for convergence study
10. Variation of (EtV/p_oRL) along edge AB with respect to number of elements
11. Variation of (EtW/p_oR^2) along edge BC with respect to number of elements
12. Variation of two lowest natural frequency with respect to number of elements
13. Plot of u, v, w vs. θ under uniform pressure (X = 12 inch)
14. Plot of u, v, w vs. x under uniform pressure ($\theta = 0°$, $\theta = 22.5°$)
15. Plot of u, v, w vs. θ for first mode (X = 12 inch)
16. Plot of u, v, w vs. θ for first mode (X = 24 inch)
17. Plot of u, v, w vs. θ for first mode ($\theta = 0°$, $\theta = 22.5°$)

18. Plot of u, v, w vs. x for first mode ($\theta = 45°$, $\theta = 67.5°$)

19. Plot of u, v, w vs. θ for second mode (X = 12 inch)

20. Plot of u, v, w vs. x for second mode ($\theta = 0°$, $\theta = 22.5°$)

21. Plot of u, v, w vs. x for second mode ($\theta = 45°$, $\theta = 67.5°$)

22. Parametric study with respect to variable X(1)

23. Parametric study with respect to variable X(2)

24. Parametric study with respect to variable X(5)

25. Parametric study with respect to variable X(6).

LIST OF SYMBOLS

E	:	Young modulus
$F(\bar{X})$	:	Objective function
g	:	Constraints
$[H]$	:	Hessian matrix
L	:	Length of a body
$[K]$, $[M]$	:	Stiffness and mass matrix respectively
$m_i, n_i, p_i, q_i, r_i, s_i$	:	Power coefficients in a polynomial
p_o	:	Pressure per unit area
R	:	Radius of curvature
r	:	Penalty parameter
S	:	Direction of descent
t	:	Thickness
u, v, w	:	Displacements in x, y and z direction
X, Y, Z	:	Global co-ordinate system
α	:	Step length
α^*	:	Optimum step length
ε	:	Strain
σ	:	Stress
ξ, η	:	Local co-ordinate system
ν	:	Possion's ratio
ω	:	Circular frequency
ρ	:	Mass density.

ABSTRACT

A computer program was developed to find the minimum weight design of a stiffened cylindrical shell under uniform internal pressure using finite element method. The constraints considered were on induced stresses displacements and natural frequency. The constant stress triangular element was chosen in preference to the more refined 36 degree of freedom element – namely the doubly curved triangle for idealisation of the shell skin, because of the limitation imposed on computer storage and time. Axial rod elements were used for idealisation of the stiffeners. Shell skin thickness and areas of stiffeners are taken as design variables. On the basis of parametric study the number of design variables was reduced. Optimisation results were sought for two different starting points. All computations were done on IBM 7044 computer.

CHAPTER 1

INTRODUCTION

With the increase in the size of modern aerospace vehicles , the demand for light weight structures also increases. This has made the structural engineers more and more conscious of minimum weight design. A structural configuration that is widely used in aerospace vehicles is the stiffened thin cylindrical shell.

Stiffened cylinders under bending are representative of aircraft fuselages whereas launch vehicles and some spacecraft can be treated as stiffened cylinders under axial compression.

Leggett and Hopkins [13] showed that sandwich shell construction becomes increasingly more efficient than stiffened panel construction as the curvature increases. Wittrick [22] investigated the optimum design of a sandwich cylinders under compression. He considered various face materials and core densities and concluded that there is a definite optimum core rigidity for each face material and design index (N/d), where N is the load d is the mean diameter of the cylinder. Joycee and Mitchell [11] determined the spacing between the stiffeners for minimum weight stiffened

cylinders. Gerard and Papirno [10] have considered the minimum weight design of ring stiffened and longitudinal stiffened cylinders under compression based on orthotropic cylinder theory. Kicher [12] treated the problem of optimum design of stiffened cylinderical shells subject to multiple load conditions.

The minimum weight design of a cylinder represents a constrained non-linear optimisation problem and is usually treated by one of the two basic mathematical programming methods, namely, the constrained technique or the direct search method and the unconstrained or the indirect method. The most widely used indirect method is the penalty function method. This method consists of solving the constrained optimisation problem as a sequence of unconstraint minimisation problems.

There are a number of ways in which the unconstrained minimisation can be accomplished. The Random search method, Univarriate method, Powell conjugate direction [17], Fletcher and Reeves conjugate gradient method [6], Quasi-Newton method [3], or Davidon-Fletcher Powell variable metric method are some of the methods that could be used. The selection of a particular method depends upon the size (i.e. number of variables) of the problem and the difficulty in computation of the gradient of the objective function. For

small size problem with a continuous function, Fletcher Reeve's conjugate gradient method or Davidon Fletcher Powell's variable métric method prove to have a faster convergence rate. The variable metric method is numerically more stable.

The numerical stability of the variable metric method depends upon the accuracy with which the minimising step length along any particular direction of descent is determined. Although the Golden section search method [4] has a slow convergence it is the most powerful technique for discontinuous functions. For continuous functions the cubic interpolation method is used for one dimensional minimisation for accuracy and faster convergence within the variable metric method.

The evaluation of the penalty function involves the evaluation of the constraints. The constraints considered in the problem are on the induced stress, natural frequencies and the maximum displacement. Thus to evaluate the constraints, a model is required to represent the structure. This model or the analytical idealisation must be accurate enough and must be suitable for embedment into the iterative design analysis loop of the optimisation procedure.

In this work, the finite element method is used. This numerical method is now widely used for structural analysis. Within this method are two approaches, namely, the force or the flexibility method and the displacement

or the stiffness method of the two, the displacement method is easier to use in automated design procedures. Zienkiewich [24] and Prezemieniecki [18] describes these methods in great detail.

Two types of elements are used to model the stiffened shell. A constant stress element is used for idealisation of the skin and axial force members for idealisation of the stiffeners. The constant stress element was selected after a comparative study was made with the doubly curved shallow shell triangle element.

The determination of all the natural frequencies is a very time consuming process. Since only the first few natural frequencies are needed, it will be a waste of computer time to evaluate all the frequencies. The static condensation is one method by which the size of the eigen-system can be reduced. As the bending degrees of freedom are predominant, the inplane degrees of freedom are removed from the eigen-system by using the equilibrium equations. Another method by which the size of the eigen problem can be reduced is the subspace iterative scheme [2]. In this method, a set of eigenvectors corresponding to the desired eigenvalues scan a subspace. By an iterative scheme, these set of eigenvectors converge to the required eigenvectors. The attraction of this scheme lies in, that in any optimisation stage the

starting set of eigenvectors are available from the previous optimisation cycle.

In this work a stiffened cylindrical shell clamped at both edges and subjected to uniform internal pressure is considered. This simplified model is considered due to the limitations on computer time and storage on IBM 7044 computer. A parametric study is conducted to find the variation of the various quantities with respect to the design parameters. The results of the parametric study are used in reducing the number of design variables in optimisation.

Optimisation results are obtained by considering the skin thickness and cross sectional areas of the stiffeners as design variables.

CHAPTER 2

FORMULATION AND SOLUTION OF THE PROBLEM

2.1 FORMULATION:

The objective is to find a minimum weight design of a cylinderical shell under uniform pressure. The behavioural constraints that must be satisfied are: (1) the stress induced must not exceed the yield strength (2) the first few natural frequencies must satisfy the specified limitations and (3) the maximum displacement must not exceed a specified value.

Mathematically the problem can be stated as follows:

$$\text{Minimise} \quad F(\bar{X}) \tag{1}$$

subject to

$$\begin{aligned} \sigma_y - \sigma_j(\bar{X}) &\geq 0 \\ \omega_k^u - \omega_k(\bar{X}) &\geq 0 \\ \omega_k(\bar{X}) - \omega_k^l &\geq 0 \\ \delta_m^u - \delta_m(\bar{X}) &\geq 0 \\ X_i &\geq 0 \end{aligned} \tag{2}$$

where

$F(\bar{X})$ = weight of the structure (objective function)

σ_y = yield strength of the material

$\sigma_j(\bar{X})$ = stress induced in the j^{th} element

$\omega_k(\bar{X})$ = k^{th} natural frequency

$\omega_k^u(\bar{X})$ = upper bound on k^{th} natural frequency

$\omega_k^L(\bar{X})$ = lower bound on k^{th} natural frequency

$\delta_m(\bar{X})$ = value of the m^{th} displacement degree of freedom

δ_m^u = upper bound on the m^{th} displacement degree of freedom

$\bar{X}$ = vector of design variables

The design variables are taken as the skin thickness and the areas of cross-section of stiffeners.

2.2 INTERIOR PENALTY METHOD OF SOLUTION:

In any optimisation problem the new design variables are found from the old design variables by the relationship

$$\bar{X}_{q+1} = \bar{X}_q + \alpha \bar{S}_q \qquad (3)$$

where

$\bar{X}_{q+1}$ = design variable vector after q+1 iterations

$\bar{X}_q$ = design variable vector after q iterations

$\bar{S}_q$ = direction of minimisation

α = step length

It is in the determination of $\bar{S}_q$ that the various techniques of optimisation differ from one another. One such method for unconstrained minimisation is to set

$$\bar{S}_q = - \nabla F(\bar{X}) \tag{4}$$

$$\text{i.e.} \quad \bar{X}_{q+1} = \bar{X}_q - \alpha \nabla F(\bar{X}) \tag{5}$$

This can also be written as

$$\frac{d\bar{X}(\alpha)}{d\alpha} = - \nabla F(\bar{X}) \tag{6}$$

$$\bar{X}(0) = \bar{X}_o$$

Thus a minimum could be obtained by solving a set of differential equations. The solution $\bar{X}(\alpha)$ is called "orthogonal trajectory" from the point $\bar{X}_o$ and it approaches a point $\nabla F = 0$ as $\alpha \rightarrow \infty$.

For unconstrained minimisation equation (6) can be modified to incorporate the influence of constraints. One approach is to add something to equation (6) which would bend the trajectory into the feasible region. This is the underlying principle of the penalty function methods [8].

A constraint divides the n-dimensional design space into two parts; the feasible region and the infeasible region. Exterior penalty method approaches the minimum from the infeasible region, while the interior penalty function

method approaches the minimum from the feasible region. In this work, the interior penalty function method is used.

The appealing feature of the interior penalty function method is that given an initial acceptable design, it produces an improving sequence of acceptable designs. Moreover we approach the constraints in this sequence in such a way that they become critical only near the end. This is a desirable feature in an engineering design process because instead of taking the optimum design we can choose a sub-optimal design but less critical design if we like. Such designs have a reserve capacity to absorb overload or abuse.

Mathematically the interior penalty function can be written as

$$\phi(\bar{X}, r) = F(\bar{X}) - r \sum_{j=1}^{m} \frac{1}{g_j(\bar{X})} \qquad (7)$$

where

r = penalty parameter

g_j = j^{th} constraint function

m = number of constraints

and $F(\bar{X})$ is to be minimised overall $\bar{X}$ satisfying $g_j(\bar{X}) \leq 0$, $j = 1,2,\ldots,m$. Note that if r is positive the effect is to add a positive penalty to $F(\bar{X})$. This is because at an interior point all terms in the sum are negative. As a

boundary of the hypersurface is approached, some g_j will approach zero and the penalty will explode. The penalty parameter r is made successively smaller in order to obtain the constrained minimum of $F(\bar{X})$.

The constraints can be normalised and the minimisation problem can be restated as follows.

Minimise $F(\bar{X})$

subject to

$$\frac{\sigma_i}{\sigma_y} - 1 \leq 0$$

$$\frac{\omega_k}{\omega_k^u} - 1 \leq 0$$

$$1 - \frac{\omega_k}{\omega_k^L} \leq 0 \qquad (8)$$

$$\frac{\delta_m}{\delta_m^u} - 1 \leq 0$$

$$- X_i \leq 0$$

The algorithm for interior penalty function method is given by the following steps.

(1) Given a starting point $\bar{X}_o$, satisfying all $g_j(\bar{X}_o) \leq 0$ and an initial value of r, minimise $\emptyset$ to obtain $\bar{X}_M$.

(2) Check for the convergence of $\bar{X}_M$.

(3) If the convergence criteria are not satisfied reduce r as $(r)_{new} = (r)_{old} c$ where $c < 1$.

(4) Take $\bar{X}_M$ as the new starting point for minimisation and repeat from step 1 onwards.

2.2.1 DAVIDON-FLETCHER POWELL METHOD:

The original inventor Davidon [5] considered this method as a terms of a variable method, some consider it as a Quasi Newton method and Fletcher and Powell [7] think it to be a conjugate direction method. This method works according to the following iterative scheme.

(1) Start with an initial $\bar{X}_o$ and an initial positive definite symmetric matrix H_o (for example the identity matrix) and set

$$S_o = - [H_o] \nabla F_o \tag{9}$$

(2) Compute $\bar{X}_{q+1} = \bar{X}_q + \alpha_q^* \bar{S}_q$ where α_q^* minimises $F(\bar{X}_q + \alpha \bar{S}_q)$. Check $\bar{X}_{q+1}$ for optimality.

(3) If $\bar{X}_{1+1}$ is not optimum, compute

$$[H_{q+1}] = [H_q] + [M_q] + [N_q] \tag{10}$$

where defining

$$[\bar{Y}_q] = \nabla F(\bar{X}_{q+1}) - \nabla F(\bar{X}_q)$$

$$[M_q] = \alpha^* \frac{S_q S_q^T}{S_q^T Y_q}$$

$$[N_q] = -\frac{(H_q Y_q)(H_q Y_q)^T}{Y_q^T H_q Y_q} \qquad (11)$$

(4) Compute $\bar{S}_{q+1} = -[H_{q+1}] \nabla F(\bar{X}_{q+1})$ and repeat from step 2.

It can be shown that if the Hessian matrix $[H_q]$ is positive definite then $[H_{q+1}]$ is also positive definite provided α_q^* is such that $\bar{S}_q^T \nabla F(\bar{X}_{q+1}) = 0$. The positive definiteness is preserved in theory only if α_q^* is the true minimum point, but round off error in other computational approximations can cause trouble. Hence in this method care must be excercised to ensure that the $[H]$ matrix is not updated with data arising from poor approximations used for computing α_q^* until $S_q^T \nabla F(\bar{X}_{q+1})$ is sufficiently small or alternatively skip the update cycle when $S_q^T \nabla F(\bar{X}_{q+1})$ is large i.e. set $[H_{q+1}] = [H_q]$ and $\bar{S}_{q+1} = [H_{q+1}] \nabla F(\bar{X}_{q+1})$ and continue as before.

Bard [1] reports that if the function is badly distorted or eccentric or if the function or the variables not properly scaled then it is possible that the elements of the matrix $[N_o]$ and $[M_o]$ would differ from one another in order of magnitudes. In finite digit arithmetic this

would imply that one of the matrices would have no contribution to the [H] matrix. This could lead to a non-positive definite matrix [H]. In such cases the most efficacious remedy would be to set [H] back to $[H_o]$ and proceed as if starting over. This resetting should not be done too often otherwise the method cannot be expected to work well. It has been recommended that it is a good practice to reset the [H] matrix after n-cycles, where n is the number of variables.

2.2.2 ONE DIMENSIONAL MINIMISATION:

In the last section it was mentioned that the D.F.P. method's stability is dependent on how accurately the minimising step length α^* is determined. Since D.F.P. requires evaluation of the gradients, it inherently assumes that the function is continuous. Hence the slope (first derivative with respect to α) information can be used for determination of α^*. The function is approximated by a cubic polynomial.

$$H(\alpha) = a + b\alpha + c\alpha^2 + d\alpha^3 \qquad (13)$$

The function and slope values at point A and B (see fig. 1) are used to determine the values of a, b, c and d.

The minimum will be at a point where $\frac{dH(\alpha)}{d\alpha} = 0$, which yields

$$b + 2c\alpha + 3d\alpha^2 = 0 \qquad (14)$$

or

$$\alpha^* = \frac{-c \pm (c^2 - 3bd)^{\frac{1}{2}}}{3d} \qquad (15)$$

As $\frac{d^2H}{d\alpha^2}$ has to be positive at the minimum, the positive sign has to be taken in Eq. (15). The constants a, b, c and d can be evaluated in terms of F(A), F(B) and F'(A) and F'(B), where F(A), F'(A) and F(B), F'(B) are the function and slope values at points A and B respectively. To ensure that $c^2 - 3bd$ is greater than zero, we have to make sure that $F'(A) < 0$ and $F'(B) > 0$. Substituting the values of a, b, c and d in equation (15) and rearranging the terms, α^* can be expressed as:

$$\alpha^* = A + \frac{F'(A) + Z + Q}{F'(A) + F'(B) + 2Z}(B - A)$$

where

$$Z^* = \frac{3(F(A) - F(B))}{(B - A)} + F'(A) + F'(B) \qquad (16)$$

$$Q = (Z^2 - F'(A)\,F'(B))^{\frac{1}{2}} \quad .$$

CHAPTER 3

ANALYSIS OF THE STRUCTURE

To evaluate the stress, displacement and frequency constraints, the analysis of the structure is required. To analyse the structure, the finite element method is used. This method consists of representing the structure by an assembly of elements as shown in Fig. 2.

Two types of elements are used to represent the shell in this work. The triangular elements are used to represent the skin and the axial force members are used to represent the stiffeners.

To represent any general shell structure accurately the doubly curved triangular elements capable of taking bending and inplane loads have to be used. However for simplicity the flat triangular elements, capable of taking constant stresses, are used in this work.

A comparative study is made here to find the relative efficiencies of a doubly curved shallow shell element [15,16] and the constant stress flat triangular element with respect to accuracy, rate of convergence and storage required. Before presenting the numerical results of the comparative study, the derivation of the stiffness and the mass matrices of the two element is outlined.

The elemental stiffness and mass matrices are derived from the local assumed displacement polynomial. Thus the finite element method may be thought of as an assumed mode analysis in which the assumed mode instead of having a uniform definition for each element has a sort of patch work of assumed modes. The assumed polynomial has a number of unknown parameters which are evaluated in terms of the nodal degrees of freedom of the element. By using the strain-displacement and stress-strain relations of linear elasticity the strain and kinetic energies of the element are expressed in terms of the unknown nodal degrees of freedom.

By expressing the strain and the kinetic energies as quadratic forms in the nodal displacement and nodal velocity vectors respectively, the element stiffness and mass matrices can be identified. The element stiffness and mass matrices are usually determined with respect to the local co-ordinate system. These matrices are then transformed to correspond to a common global co-ordinate system before assembling the structural stiffness and mass matrices. The assembled stiffness and mass matrices are used to state the equilibrium and the eigenvalue problems in the standard manner.

3.1 DOUBLY CURVED TRIANGLE (D.C.T.):

The geometry of an arbitrary triangular shallow shell element is shown in Fig. 3.

Here u, v and w are the displacements in the local co-ordinate system ξ, η, Z and X, Y, Z represents the global co-ordinate system. The dimensions a, b and c and the rotation angle θ are defined in terms of the global co-ordinates of the vertices. $f(\xi, \eta)$ defines the shape of the shell about the base plane $\xi - \eta$.

3.1.1 STIFFNESS MATRIX:

From the shallow shell theory of Novozhilov [14], the strain energy is given by

$$U = \frac{Et}{2(1-\nu^2)} \iint \Big\{ u_\xi^2 + v_\eta^2 + 2\nu u_\xi v_\eta + \frac{1}{2}(1-\nu)(u_\eta + v_\xi)^2 - 2\big[(f_{\xi\xi} + \nu f_{\eta\eta})u_\xi + (f_{\eta\eta} + \nu f_{\xi\xi})v_\eta + (1-\nu) f_{\xi\eta} (u_\eta + v_\xi)\big] w + \big[(f_{\xi\xi}^2 + f_{\eta\eta}^2 + 2\nu f_{\xi\xi} f_{\eta\eta} + 2(1-\nu) f_{\xi\eta}^2\big] w^2 + \frac{t^2}{12}\big[w_{\xi\xi}^2 + w_{\eta\eta}^2 + 2\nu w_{\xi\xi} w_{\eta\eta} + 2(1-\nu) w_{\xi\eta}^2\big]\Big\} d\xi\, d\eta \qquad (17)$$

where the integration is to be done over the base plane 1'2'3'. The subscripts of u, v, w and f represents the

derivatives with respect to ξ and η. For example

$$u_\xi = \frac{\partial u}{\partial \xi}, \qquad w_{\xi\eta} = \frac{\partial^2 w}{\partial \xi \partial \eta} \qquad \text{etc.}$$

The function $f(\xi,\eta)$ is assumed to be of quadratic form:

$$f(\xi,\eta) = c_1 + c_2\xi + c_3\eta + c_4\xi^2 + c_5\xi\eta + c_6\eta^2 \qquad (18)$$

This implies that the shell element has constant curvatures and this is consistent with the shallow shell theory.

A quantic polynomial is assumed for the normal displacement w and a cubic polynomial for the tangential displacement. Thus the tangential and the normal displacement yield the same energy convergence rate n^{-6} where n is the number of elements.

$$u(\xi,\eta) = a_1 + a_2\xi + a_3\eta + a_4\xi^2 + a_5\xi\eta + a_6\eta^2 + a_7\xi^3 + a_8\xi^2\eta + a_9\xi\eta^2 + a_{10}\eta^3 \qquad (19a)$$

$$v(\xi,\eta) = a_{11} + a_{12}\xi + a_{13}\eta + a_{14}\xi^2 + a_{15}\xi\eta + a_{16}\eta^2 + a_{17}\xi^3 + a_{18}\xi^2\eta + a_{19}\xi\eta^2 + a_{20}\eta^3 \qquad (19b)$$

$$w(\xi,\eta) = a_{21} + a_{22}\xi + a_{23}\eta + a_{24}\xi^2 + a_{25}\xi\eta + a_{26}\eta^2 + a_{27}\xi^3 + a_{28}\xi^2\eta + a_{29}\xi\eta^2 + a_{30}\eta^3 + a_{31}\xi^4 + a_{32}\xi^3\eta + a_{33}\xi^2\eta^2 + a_{34}\xi\eta^3 + a_{35}\eta^4 + a_{36}\xi^5 + a_{37}\xi^3\eta^2 + a_{38}\xi^2\eta^3 + a_{39}\xi\eta^4 + a_{40}\eta^5 \qquad (19c)$$

The nodal displacement degree of freedom for $u(\xi,\eta)$ and $v(\xi,\eta)$ are taken as u and v and their first derivatives with respect to ξ and η at each of the corners plus u and v at the centroid of the element. This gives a total of 20 degrees of freedom for the element consistent with the 20 free parameters in equation (19a) and (19b). The nodal displacements for $w(\xi,\eta)$ are taken as w and its first and second derivatives with respect to ξ and η at each of the three corners. These along with the constraint that the normal must be cubic in variation along the edges, yield sufficient information for evaluating the 20 free parameters of (19c). All generalised displacement are assembled into a 38 column vector $\{W_1\}$ in local co-ordinate system ξ, η as

$$\{W_1\}^T = (u_1, u_{\xi 1}, u_{\eta 1}, v_1, v_{\xi 1}, v_{\eta 1}, w_1, w_{\xi 1}, w_{\eta 1}, w_{\xi\xi 1}, w_{\xi\eta 1}, w_{\eta\eta 1}, u_2 \cdots u_3, \ldots, u_c, v_c) \qquad (20)$$

The subscripts 1, 2, 3 and c denotes the corners 1, 2 and 3 and the centroid of the element respectively. The coefficients a_i of equations (19) are assembled into a column vector $\{A\}$ as

$$\{A\}^T = (a_1, a_2, \ldots, a_{40}) \tag{21}$$

Combining equations (19) to (21) one obtains

$$\begin{Bmatrix} W_1 \\ 0 \\ 0 \end{Bmatrix} = [T]\{A\} \tag{22}$$

where the 40 x 40 T matrix is given in Appendix A. The determinant of T has a value $-64c^{34}(a + b)^{31}(a^2 + c^2)(b^2 + c^2)/729$ which is non-zero for all practical problems. Hence the equation (22) may be inverted to obtain

$$\{A\} = [T^{-1}] \begin{Bmatrix} W_1 \\ 0 \\ 0 \end{Bmatrix} = [T_1]\{W_1\} \tag{23}$$

where the 40 x 38 matrix $[T_1]$ consists of the first 38 columns of $[T^{-1}]$.

The displacement functions of equations (19) can be rewritten as

$$u = \sum_{j=1}^{10} a_j \xi^{m_j} \eta^{n_j}$$

$$v = \sum_{j=11}^{20} a_j \xi^{p_j} \eta^{q_j} \qquad (24)$$

$$w = \sum_{j=21}^{40} a_j \xi^{r_j} \eta^{s_j}$$

By substituting the displacement function of Eq. (24) into the strain energy expression (17), and performing the integration, the strain energy can be expressed in matrix form as

$$U = \frac{Et}{2(1-\nu^2)} \{A\}^T [k] \{A\} \qquad (25)$$

where the elements of the 40 x 40 matrix $[k]$ are given in Appendix A. Combining equations (23) and (25), the strain energy can be obtained in terms of $\{W_1\}$ as

$$U = \frac{Et}{2(1-\nu^2)} \{W_1\} [K_1] \{W_1\} \qquad (26)$$

where $[K_1] = [T_1]^T [k] [T_1]$ is the 38 x 38 stiffness matrix in terms of the generalised displacements relative to local co-ordinate system using the relation. The stiffness matrix relative to the global co-ordinate system can be obtained using the relation

$$\{W_1\} = [R]\{W_2\} \tag{27}$$

where

$$\{W_2\}^T = (u_1, u_{x1}, u_{y1}, v_1, v_{x1}, v_{y1}, w_1, w_{x1}, w_{y1}, w_{xx1}, w_{xy1}, w_{yy1}, u_2, \ldots, u_3, \ldots, u_c, v_c) \tag{28}$$

where $\{W_2\}$ is the generalised displacement vector relative to the global co-ordinates and $[R]$ is the rotation matrix given in Appendix A. Equation (26) and (27) yield

$$u = \frac{Et}{2(1-\nu^2)} \{W_2\}^T [K_2] \{W_2\} \tag{29}$$

where the matrix

$$[K_2] = [R]^T [T_1]^T [k] [T_1] [R] \tag{30}$$

is the 38 x 38 stiffness matrix relative to the global co-ordinate system.

3.1.2 CONSISTENT LOAD VECTOR:

The consistent load vector is obtained by calculating the virtual work done by the applied loads. $Q_u(\xi,\eta)$, $Q_v(\xi,\eta)$ and $Q_w(\xi,\eta)$ in the u, v and w directions respectively. The transformed load vector becomes

$$\{P\} = [R]^T [T_1]^T \{Q\} \tag{31}$$

where the entries of $\{Q\}$ are given by

$$Q_i = \begin{cases} \iint Q_u \, \xi^{m_i} \, \eta^{n_i} \, d\xi \, d\eta & i \leq 10 \\ \iint Q_v \, \xi^{p_i} \, \eta^{q_i} \, d\xi \, d\eta & 10 < i \leq 20 \\ \iint Q_w \, \xi^{r_i} \, \eta^{s_i} \, d\xi \, d\eta & 20 < i \leq 40 \end{cases} \tag{32}$$

In the case of a uniform pressure load of intensity Q_o,

$$Q_i = \begin{cases} 0 & i \leq 20 \\ - Q_o \, F(r_i, s_i) & i > 20 \end{cases} \tag{33}$$

The centroidal displacement degrees u_c and v_c are condensed out as they lie inside the element. This reduces the number of degree of freedom in each element and also simplifies the assembly procedure. The reduction is carried out as follows.

The elemental equilibrium equations can be written in partitioned form as

$$[K_2]\{W_2\} = \left[\begin{array}{c|c} K_o & K_{oc} \\ \hline K_{oc}^T & K_c \end{array}\right] \left\{\begin{array}{c} W_o \\ \hline W_c \end{array}\right\} = \left\{\begin{array}{c} P_o \\ \hline P_c \end{array}\right\} \tag{34}$$

where $\{W_c\}$ is a 2 component vector (u_c, v_c) and $\{W_o\}$ contains the first 36 component of equation (28). Equation (34) can be written as two separate equations and W_c can be determined to obtain

$$[K]\{W\} = \{P\} \tag{35}$$

where

$$[K] = [K_o] - [K_{oc}][K_c^{-1}][K_{oc}]^T \tag{36}$$

is the reduced 36 x 36 stiffness matrix and

$$\{P\} = \{P_o\} - [K_{oc}][K_c^{-1}]\{P_c\} \tag{37}$$

is the reduced consistent load vector.

3.1.3 MASS MATRIX:

The kinetic energy of the shell element can be expressed as

$$T = \frac{\rho t}{2} \int\int (\dot{u}^2 + \dot{v}^2 + \dot{w}^2) d\xi \, d\eta \tag{38}$$

As the shell vibrations involve predominantly normal motion, within the domain of small deformation theory the tangential inertia can be neglected. Assuming harmonic time dependence, Eq. (38) can be written as

$$T = \frac{\rho t \omega^2}{2} \int\int w^2 \, d\xi \, d\eta \tag{39}$$

where ω is the circular frequency. Substitution of Eq. (24) into Eq. (39) yields

$$T = \frac{\rho\omega^2}{2} \{A\}^T [m] \{A\} \tag{40}$$

where

$$\begin{aligned} m_{ij} &= F(m_i + m_j,\ n_i + n_j) && i > 20,\ j > 20 \\ &= 0 && i < 20,\ j < 20 \end{aligned} \tag{41}$$

Following the same transformation procedure described for the stiffness matrix, the elemental mass matrix in global co-ordinate system can be obtained as

$$[M] = [R]^T [T_1]^T [m] [T_1] [R] \tag{42}$$

3.2 CONSTANT STRESS FLAT TRIANGULAR ELEMENT (C.S.T.):

This element has a constant stress field within the element. By Hook's law therefore the strains are also constant. From strain displacement relationship we get a linearly varying displacement field. It is also assumed that the element can only undergo inplane displacement as shown in Fig. 4.

3.2.1 STIFFNESS MATRIX:

The local displacement variation can be assumed as

$$u(\xi, \eta) = a_1 + a_2 \xi + a_3 \eta \tag{43a}$$

$$v(\xi, \eta) = a_4 + a_5 \xi + a_6 \eta \tag{43b}$$

The constants in Eq. (43) can be evaluated in terms of the nodal displacement degree of freedom and the nodal co-ordinates and Eq. (44) can be written in matrix form as

$$\begin{Bmatrix} u \\ v \end{Bmatrix} = [A] \{W_1\} \tag{44a}$$

where the elements of the matrix $[A]$ is given in Appendix B and $\{W_1\}$ is the vector of generalised displacement relative to the local co-ordinates

$$\{W_1\} = \{u_1, v_1, u_2, v_2, u_3, v_3\} \tag{44b}$$

The strains can be obtained by differentiating equation (44) to yield

$$\{\epsilon\}^T = [b] \{W_1\} \tag{45}$$

where the matrix $[b]$ is given in Appendix B and $\{\epsilon\}^T$ is the strain vector $\{\epsilon_{zz}, \epsilon_{\eta\eta}, \epsilon_{z\eta}\}$

By Hook's law the stresses can be written as

$$\{\sigma\} = [c] \{\epsilon\} \tag{46}$$

where the 3 x 3 matrix $[c]$ is given in Appendix B and

is the stress vector

The strain energy of the element is given by

$$U = \frac{t}{2} \iint \{\varepsilon\}^T \{\sigma\} \, d\xi \, d\eta \tag{47}$$

By substituting equations (45) and (46) in equation (47), the strain energy can be written as

$$U = \frac{t}{2} \iint \{W_1\}^T [b]^T [c] [b] \{W_1\} \, d\xi \, d\eta \tag{48}$$

As the matrices $[b]$ and $[c]$ and the vector $\{W_1\}$ are constants, they can be taken out of the integral and the integration can be performed to obtain

$$U = \frac{1}{2} \{W_1\}^T [K_1] \{W_1\} \tag{49}$$

where the 6 x 6 matrix

$$[K_1] = \Delta t [b]^T [c] [b] \tag{50}$$

is the stiffness matrix relative to the local system and Δ is the area of the triangle.

This matrix is now transformed to the global co-ordinate system using

$$\{W_1\} = [R] \{W_2\} \tag{51}$$

where the 9 x 6 matrix $[R]$ is given in Appendix B and

$$\{W_2\}^T = \{u_1, v_1, w_1, u_2, \ldots, u_3 \ldots\}^T \qquad (52)$$

is a vector of generalised displacements relative to the global co-ordinate system.

Substitution of Eq. (51) in Eq. (49) yields

$$[K_2] = [R]^T [K_1] [R] \qquad (53)$$

where the 9 x 9 matrix $[K_2]$ is the stiffness matrix relative to the global system.

3.2.2 MASS MATRIX:

The kinetic energy of the element is given by

$$T = \frac{1}{2} \int t \iint (\dot{u}^2 + \dot{v}^2) \, d\xi \, dr \qquad (54)$$

Assuming a harmonic time dependence and substitution of Eq. (43) into Eq. (54), one can express the kinetic energy as

$$T = \frac{\omega^2}{2} \{W_1\}^T [m] \{W_1\} \qquad (55)$$

where the 6 x 6 matrix $[m]$ is the mass matrix relative to the local co-ordinate system and is given in Appendix B, and ω is the circular frequency.

Following the same transformation procedure as given for the stiffness matrix, the 9 x 9 mass matrix $[M]$

relative to the global co-ordinate system can be obtained as

$$[M] = [R]^T [m] [R] \tag{56}$$

3.3 EVALUATION OF CONSTRAINTS:

Once the elemental stiffness and mass matrices are available, the stiffness and mass matrices of the whole structure can be obtained [18,24]. After introducing the boundary conditions, the displacement and the natural frequencies can be obtained respectively by solving the two system of equations:

$$[K]\{W\} = \{P\} \tag{57}$$

$$([K] - \omega^2 [M])\{W\} = 0 \tag{58}$$

where $[K]$ and $[M]$ are the structural stiffness and mass matrices respectively, $\{W\}$ is the displacement vector and $\{P\}$ the external load vector and ω is the circular frequency.

Once the displacements are known the stresses can be calculated. The principal stresses are found and Von-misses yield criterion is used to evaluate the stress constraint.

To evaluate the natural frequencies, the subspace iteration scheme described in the following section is used.

3.4 SUBSPACE ITERATIVE SCHEME [2]:

The objective is to solve for p-lowest eigenvalues and the associated eigenvectors satisfying the relation

$$[K]\{\phi\} = [M]\{\phi\}[\Omega^2] \tag{59}$$

where $\{\phi\}$ stores a set of p-eigenvector corresponding to the frequencies ω_i; $[\Omega^2]$ is a diagonal matrix $[\Omega^2] = [\omega_i^2]$ where ω_i are the rotational frequencies.

The essential idea is to iterate simultaneously with p-linearly independent vectors which initially span the starting subspace S_o, until S_∞ is spanned. The required eigenvectors are then computed without further iterations. The total number of required iterations depends upon how close S_o is to S_∞. But the effectiveness of the algorithm lies in that it is easier to establish p-dimensional starting subspace S_o close to S_∞ than to find p-vectors, each of which is close to the required eigenvectors. Also convergence of subspace is all that is required and not of individual iteration vectors to the eigenvectors.

The algorithm is given by the following steps:

(1) Let $\{X_o\}$ store the set of p-eigenvectors corresponding to the natural frequencies desired.

(2) Solve the set of simultaneous equation

$$[K]\{\bar{X}_k\} = M\{X_{k-1}\} \tag{60}$$

(3) Find the projection of the operations $[K]$ and $[M]$ onto S_k

$$[K]_k = \{\bar{X}_k\}^T [K] \{\bar{X}_k\} \tag{61}$$

$$[M]_k = \{\bar{X}_k\}^T [M] \{\bar{X}_k\} \tag{62}$$

(4) Check for convergence i.e. $[M_k] = [I]$ i.e. identity matrix.

(5) Solve for the eigensystem of the projected operators

$$[K_k]\{Q_k\} = [M]_k \{Q_k\} \Omega_k^2 \tag{63}$$

(6) Find an improved approximation to the eigenvectors

$$X_k = \bar{X}_k Q_k$$

and return to step 2.

Then provided S_o is not orthogonal to one of the required eigenvectors

$\Omega_k^2 \rightarrow \Omega^2$; $X_k \rightarrow \emptyset$ as $k \rightarrow \infty$ is obtained.

Assuming that S_k is close to S_∞, the convergence rate of the i^{th} column in X_k is $\omega_i^2/\omega_{p+1}^2$. Although this is an asymptotic convergence rate, it indicates that the lowest eigenvalue converges at the fastest rate. As the

vectors span S_k, they become more and more parallel and hence form poorer and poorer basis. One way to overcome this difficulty is to generate orthogonal bases in the subspace S_k. Another way to accelerate the convergence is to choose q eigenvectors with $q \geq p$ and to stop the iteration process whenever p of the eigenvectors have converged. The originator of this method Bathe and Wilson [2], recommended a value of $q = \min (2p, p+8)$.

To find the starting subspace, the following is the recommendation of Bathe and Wilson [2]. The first column of MX_o (Eq. (60)) is set equal to the diagonal elements of [M]. This assures that all degree of freedom corresponding to the natural frequencies are excited in order not to miss a mode. The other columns are not vectors with +1 at the co-ordinates with the largest m_{ii}/k_{ii} ratio.

3.5 COMPARATIVE STUDY:

A comparative study between constant stress triangular element (C.S.T.) and doubly curved triangular element was made using a simply supported spherical cap shown in Fig. 5, as a test problem. The cap was subjected to uniform pressure. As the structure and the loads on it are symmetric in nature only one quarter of the cap is taken. The idealisation of the structure using D.C.T. and C.S.T. are shown in Fig. 6(a) and 6(b) respectively.

Sixty three degrees of freedom were taken for the idealisation with D.C.T. and seventyfive degrees of freedom for the idealisation with C.S.T. The non-dimensional parameters (Etv/p_oRL) and (Etw/p_oR^2) are plotted along the edge AB and BC (see Fig. 5) respectively in Fig. 7 and 8 From the plots it is apparent that even with lesser degree of freedom D.C.T. gives more accurate results than C.S.T.

The execution time on IBM 7044 computer using D.C.T. for idealisation for one static analysis and one dynamic analysis for the two lowest frequencies was found to be 5 minutes 3 seconds, while for C.S.T. it was found to be 51 seconds. Now on an average, an optimisation problem requires nearly 600 function evaluation (Ref. [12]). Thus only time consideration prohibits the use of D.C.T. for idealisation of the skin of the shell.

The other problem with D.C.T. is that of storage. D.C.T. has twelve degrees of freedom per node, while C.S.T. has three degrees of freedom per node. Thus for every node of D.C.T., four nodes of C.S.T. can be taken. Now in an idealisation of the stiffened shell the most convenient idealisation is that of placing a node at the intersection of a circumferential and longitudinal stiffener. Ref. [12] reports that near the optimum shell design, the longitudinal stiffeners are separated by two or three degrees from

each other. Thus the number of nodes can be very high and hence the storage problem in case of D.C.T. will be very severe.

Thus even though D.C.T. yields more accurate results than C.S.T., the time and storage consideration shows that C.S.T. should be used for idealisation of the shell skin.

3.6 CONVERGENCE STUDY OF C.S.T.:

For the spherical cap problem a number of idealisation were made as shown in Fig. 9. The variation of the non-dimensional displacements (EtV/RL) and (EtW/R^2) (along the edge AB and BC respectively) with the number of elements are plotted in Fig. 10 and 11 respectively. For the idealisation with elements 4, 6 and 8, the results obtained are found to have no relation with the solution and hence are not plotted. The plot in Fig. 10 and 11 show that with the increase in number of elements, the results tends towards the exact solution. In Fig..12, the variation of the two lowest natural frequencies with the number of elements are plotted. From Fig. 10, 11 and 12 it can be seen that the structure becomes less stiffer with the increase in number of elements.

The number of elements is inversely proportional to the step size (length for one dimensional elements, area

for two dimensional element and volume for three dimensional element). As the number of elements increases the step size decreases. The truncation error (in this case the difference between the actual mode shape and the mode shape obtained from the patch work of the approximated mode shape of element) decreases with the decrease in step size. But the round off error caused by the finite digit arithmetic of the computer, increases with the decrease in step size. To obtain the optimum number of elements which would yield the minimum error, the results must be plotted against the number of elements and that point should be taken where the results do not change appreciably with the change in number of elements. Unfortunately this could not be done as the storage limitation of IBM 7044 computer is 32 K bits. Hence the absolute values of displacements, stresses and frequencies must be taken with caution. Yet behaviour of these quantities at any node with respect to other nodes can be taken. Also the behaviour of these quantities with respect to design parameters can be taken. For in both the cases the effect of the error would be uniform.

CHAPTER 4

RESULTS AND DISCUSSIONS

In any optimisation problem, the time consuming operation is the function evaluation. A function evaluation requires the analysis of the structure. To save computer time, the displacements and frequencies are linearised over a small domain of the design variables, thereby avoiding the regular function evaluation until the design variables change by a certain percentage.

4.1 DISPLACEMENTS AND NATURAL FREQUENCY GRADIENTS:

Assuming that the load vector is independent of the design variables and the mode shapes change very little with a small change in the design variables, Eqs. (57) and (58) can be differentiated with respect to the design variables to yield.

$$\frac{\partial [K]}{\partial \bar{X}} \{W\} + [K] \frac{\partial \{W\}}{\partial \bar{X}} = 0 \qquad (64)$$

$$\left(\frac{\partial [K]}{\partial \bar{X}} - 2\omega \frac{\partial \omega}{\partial \bar{X}} - \omega^2 \frac{\partial [M]}{\partial \bar{X}}\right) \{W\} = 0 \qquad (65)$$

Premultiplying Eqs. (64) by $[K^{-1}]$ and Eqs. (65) by $\{W\}^T$ and rearranging the terms one obtains.

$$\frac{\partial \{W\}}{\partial \bar{X}} = -\left[K^{-1}\right] \frac{\partial [K]}{\partial \bar{X}} \{W\} \tag{66}$$

$$\frac{\partial \omega}{\partial \bar{X}} = \frac{\{W\}^T \frac{\partial [K]}{\partial \bar{X}} \{W\} - \omega^2 \{W\}^T \frac{\partial [M]}{\partial \bar{X}} \{W\}}{2\omega \{W\}^T [M] \{W\}} \tag{67}$$

Thus the evaluation of the displacement and frequency gradients require the evaluation of $\frac{\partial [K]}{\partial \bar{X}}$ and $\frac{\partial [M]}{\partial \bar{X}}$. The evaluation of $\frac{\partial [K]}{\partial \bar{X}}$ and $\frac{\partial [M]}{\partial \bar{X}}$ requires the assembly of the stiffness and mass matrices at the perturbed point if a finite difference scheme is used. Thus we do not have to solve an eigenvalue system or a set of simultaneous equations to evaluate the natural frequency and displacement gradients. Once these gradients are known, they are assumed constant over a small domain of the design variables and the displacement and frequencies are calculated directly using the relations.

$$\{W\}_{new} = \{W\}_{old} + \sum_{i=1}^{n} \Delta x_i \frac{\partial \{W\}}{\partial x_i} \tag{68}$$

$$\omega_{new} = \omega_{old} + \sum_{i=1}^{n} \Delta x_i \frac{\partial \omega}{\partial x_i} \tag{69}$$

4.2 CYLINDRICAL SHELL PROBLEM:

The problem considered is the minimum weight design of a thin cylindrical shell clamped at both ends and subjected to a uniform pressure as shown in Fig. 2. The skin of the shell is idealized by constant-stress triangular elements and the stiffeners byaxial rod elements as shown in Fig. 1. The design variables are skin thickness and the cross sectional areas of the stiffeners. The constraints are placed on the induced stresses, natural frequencies and displacements.

As the structure and loads are symmetric in nature only one quarter of the shell is considered*. The objective is to minimise the function

$$F(\bar{X}) = \rho\pi RL\, X(1) + \rho L \sum_{i=1}^{M} X(i+1) + \rho\pi R \sum_{j=M+1}^{M+N} X(j+1) / \rho\pi RL \qquad (70)$$

where

X(1) = skin thickness

X(i+1) for i = 1,N = Longitudinal stiffener areas

X(j+1) for j = M+1, M+N are circumferential stiffner areas

M = number of longitudinal stiffeners

N = number of circumferential stiffeners

---

* At X = 0 and L, u, v and w are zero; At Z = 0, V is zero; and at Y = 0, w is zero.

The upper bound on the natural frequencies and displacements are taken as thirty percent more than the values calculated at the starting point.

4.2.1 PARAMETRIC STUDY:

A parametric study is conducted for a stiffened cylindrical shell with five longitudinal and four circumferential stiffeners in a quarter shell. In Figures 13 to 21 are plotted the displacements and mode shapes at the reference point. The reference point is taken as

X(1) = 0.004 inches

X(2) = 0.010 inches

X(3) = 0.010 inches

X(4) = 0.010 inches

X(5) = 0.040 inches

X(6) = 0.040 inches

E = 10^7 psi

ρ = 0.101 lbs/cubic inch

ν = 0.333

R = 150 inches

L = 60 inches

Figure 13 is a plot of u, v and w vs. θ at x = 12" for a uniform pressure load of 3 psi. The displacements are sinusodial in nature. The variation of

displacements u has a wavelength of π radians while the wavelength for displacements v and w is 2π radians. The displacement v and w vary with a phase difference of $\pi/2$. This phase difference is in accordance with the boundary conditions imposed due to symmetric nature of the problem. The boundary conditioned imposed are that the displacements v and w become alternatively zero after each angular rotation of $\pi/2$. Hence the phase difference between v and w must be an integer multiple of $\pi/2$.

Figure 14 is a plot of u, v and w vs. x at $\theta = 0°$ and 22.5°. These plots show that the nature of variation of u, v and w vs. θ is sinusodial in nature for any given value of x, but the magnitude of the amplitude varies. The variation of the amplitude is symmetric about the mid section. that is x = 30 inches. This is also expected in this case as the structure and the loading are symmetric about the mid sections.

Figures 15 to 18 are the plots for the first mode of vibration. The natural frequency for the first mode of vibration was found to be 89.7 cycles per second. The displacements v and w are out of phase by $\pi/2$ radians.

Figures 19 to 21 are the plots for the second mode of vibration. The natural frequency for the second mode of vibration was found to be 92.3 cycles per second.

The results show that the phase difference between the displacements v and w is $3\pi/2$ radians.

Figures 22 to 25 show the plots of the displacements and frequency versus the design variables. The numerical values are given in Table 3.

From Figure 22 it is seen that with the variation of skin thickness, X(1), by 36 percent the variation in the displacements u, v and w are 32, 18.2 and 18.2 percent respectively.

Figure 23 shows that with a variation of area of longitudinal stiffeners, X(2), by 45 percent the variation of the displacement u is of the order of 2 percent. The displacements v and w are practically unaffected. The variation of the other longitudinal stiffener areas do not affect the results appreciably. This shows that for a shell under uniform pressure, the longitudinal stiffeners have a negligible effect.

Figure 24 indicates that with a variation of the area of circumferential stiffeners, X(5), by 36 percent, the displacements u, v and w vary by 1.7, 2.7 and 2.7 percent respectively. Figure 25 shows that with variation of X(6) by 36 percent the variation in the displacements u, v and w are 13.0, 11.8 and 11.8 percent respectively. These results show that the circumferential stiffeners

located farther away from the ends of a cylinder affect the results to a greater extent compared to the one located near the ends. The variation in the two lowest natural frequencies is negligible.

4.2.2 Minimum weight design:

A number of numerical difficulties were encountered in the solution of the optimisation problem. Initially the problem was worked with six design variables. The first difficulty that arose was due to the approximate evaluation of the displacements and natural frequencies using equations (68) and (69). Towards the end of one dimensional minimisation the program got bogged down as the computer was evaluating the function at two points only. These points were separated by a distance equal to the domain over which the displacements and frequencies were approximated. This difficulty was overcome by reducing the domain of approximation after every five iterations. Inspite of this the convergence was so slow that not even one unconstrained minimisation could be done in 30 minutes of computer time. To accelerate the process, the number of design variables was reduced to three. This was done by assuming the area of cross section of all longitudinal

stiffeners to be same. A similar assumption was made for the circumferential stiffeners. This increased the convergence rate slightly but a new difficulty arose.

Though the penalty function was decreasing the objective function was increasing. Two steps were taken to overcome this. The initial value of the penalty parameter was decreased and the variables were non-dimensionalized with respect to the length of the starting design vector. After an initial rise in objective function, the value started decreasing and at the end of 30 minutes a 20 percent reduction in the objective was found and all displacement constraints were activated. The starting and the final values of optimisation are given in Table 4.1. In Table 4.2 the initial values and the final results of optimisation, obtained with a different starting point are given. The upper bounds on the displacements and natural frequencies are taken as 30 percent more than the values corresponding to the starting point. In both these examples, fourteen constraints were considered. The first seven constraints were on induced stresses. The next four were on the natural frequencies. g(12), g(13) and g(14) are constraints on the displacement u, v and w respectively.

CHAPTER 5

CONCLUSIONS AND RECOMMENDATIONS

5.1 CONCLUSIONS:

The results presented in this work show that whenever finite element method is used the optimum number of elements which would yield a minimum error, should be determined. In case this is not done the error in the analysis results may be as high .50 to 60 percent.

The variation of crosssectional area of longitudinal stiffners have a negligible effect on the stresses, displacements and frequencies for a shell under uniform pressure.

The circumferential stiffeners located further away from the ends of the cylinder have a greater effect on displacements and stresses than the ones located near the ends.

5.2 RECOMMENDATIONS:

In this work the buckling and flutter constraints were not included. To include these constraints the spacing of stiffeners must also be taken as variables. If an optimum is sought, considering these

constraints, then near the optimum, the spacing between the longitudinal stiffeners will be of the order of two to three degrees (Ref. [12]). Since the most convenient idealisation involves the placing of nodes at the intersection of longitudinal and circumferential stiffeners, this will require a very large number of elements. This would require a large amount of computer storage and time for the analysis of the structure. This is the reason why a a simplified model was chosen in the present analysis. This difficulty can be surmounted by taking the following steps. Instead of using two types of isotropic elements for idealisation, use an orthotropic shell element. This element could be obtained by averaging the elastic properties of stiffeners over the stiffener spacings. This would help in reducing the number of elements for idealisation. By using sparse matrix method instead of band width method, the severity of storage and computer time problem could be reduced.

To save the computer time further the optimisation technique presented in Ref. [23] is recommended. In this scheme the optimum is sought in two stages. First, by a proper grouping of the design variables, the number of parameters that optimise the weight is minimised. On the basis of this, a mathematical search technique is

employed, and design charts are prepared which clearly show that the effect of these few parameters on the weight of the shell.

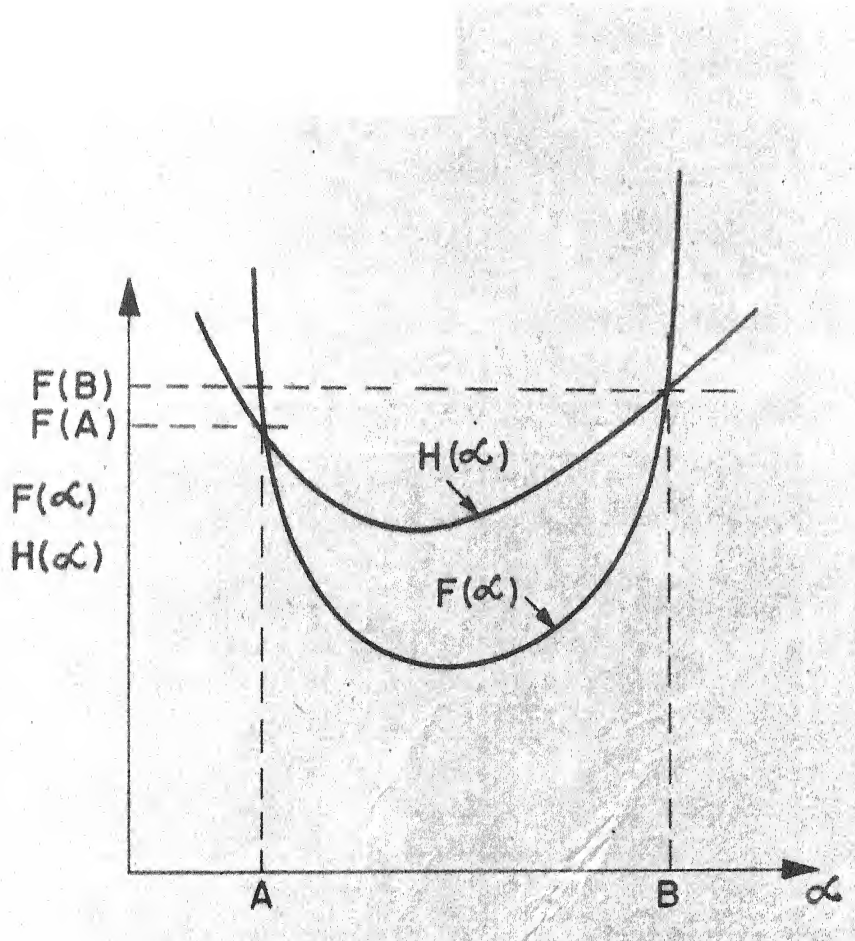

Fig. 1 Schematic Diagram Of Cubic Interpolation

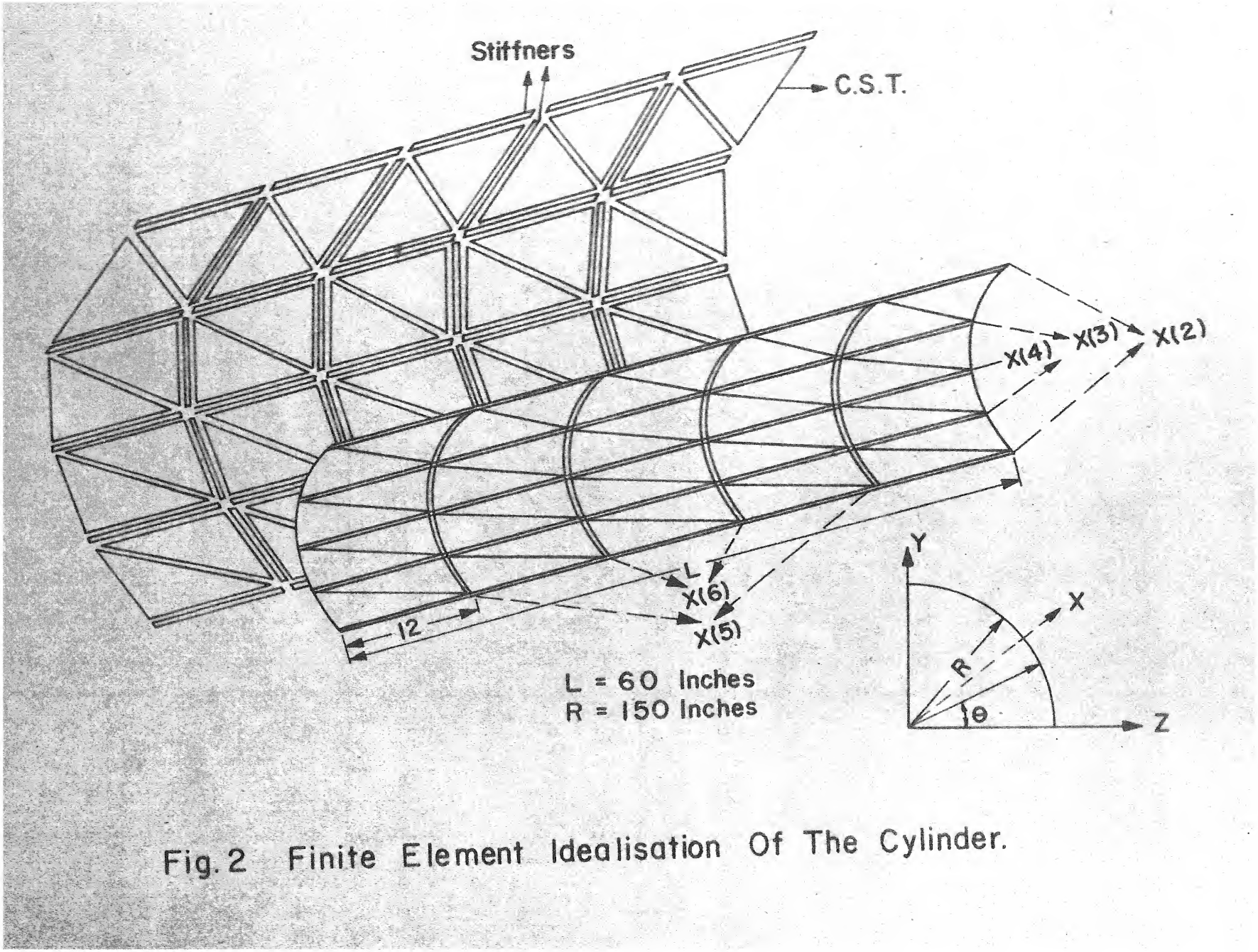

Fig. 2 Finite Element Idealisation Of The Cylinder.

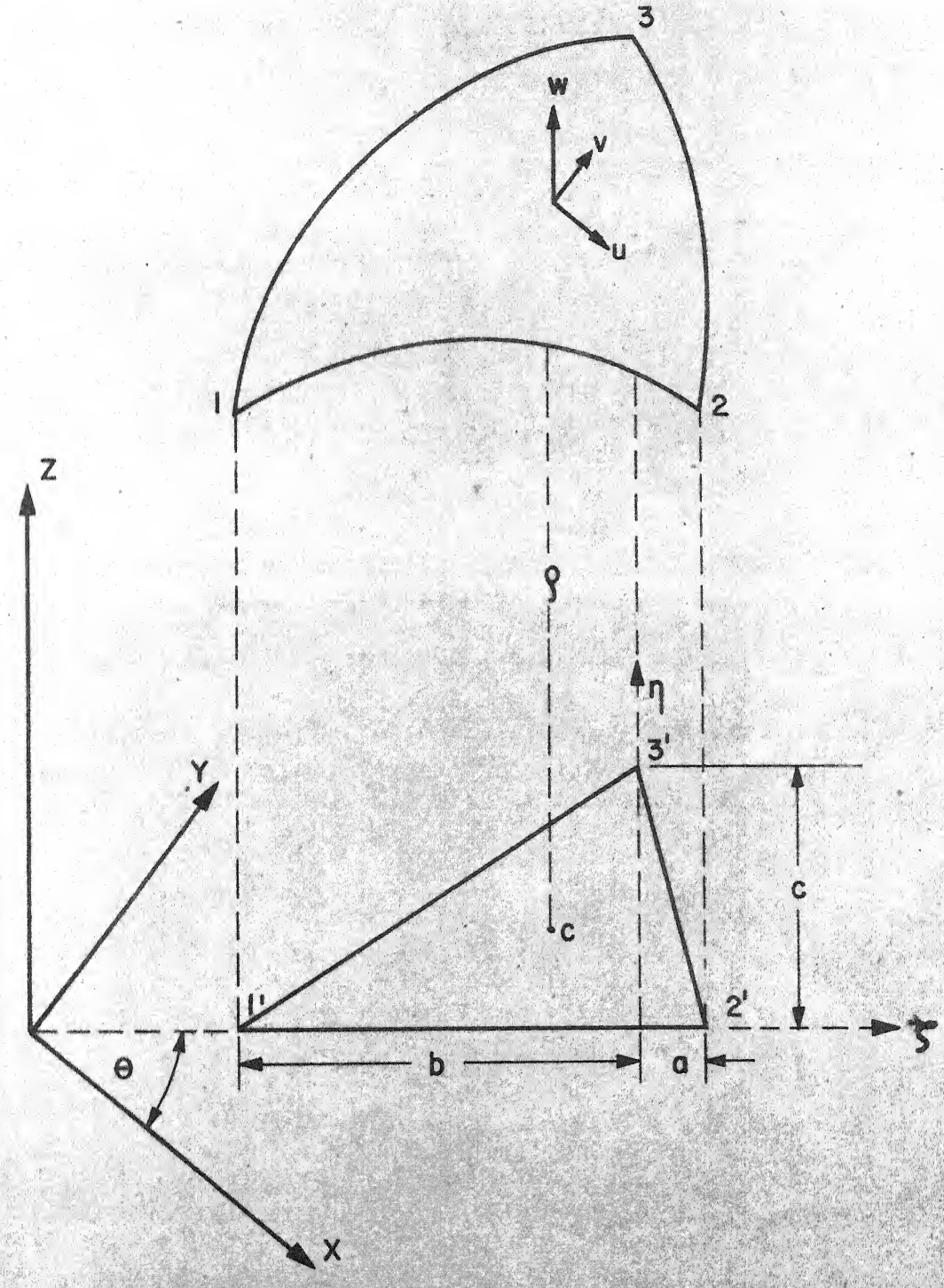

Fig.3 Doubly Curved Triangle

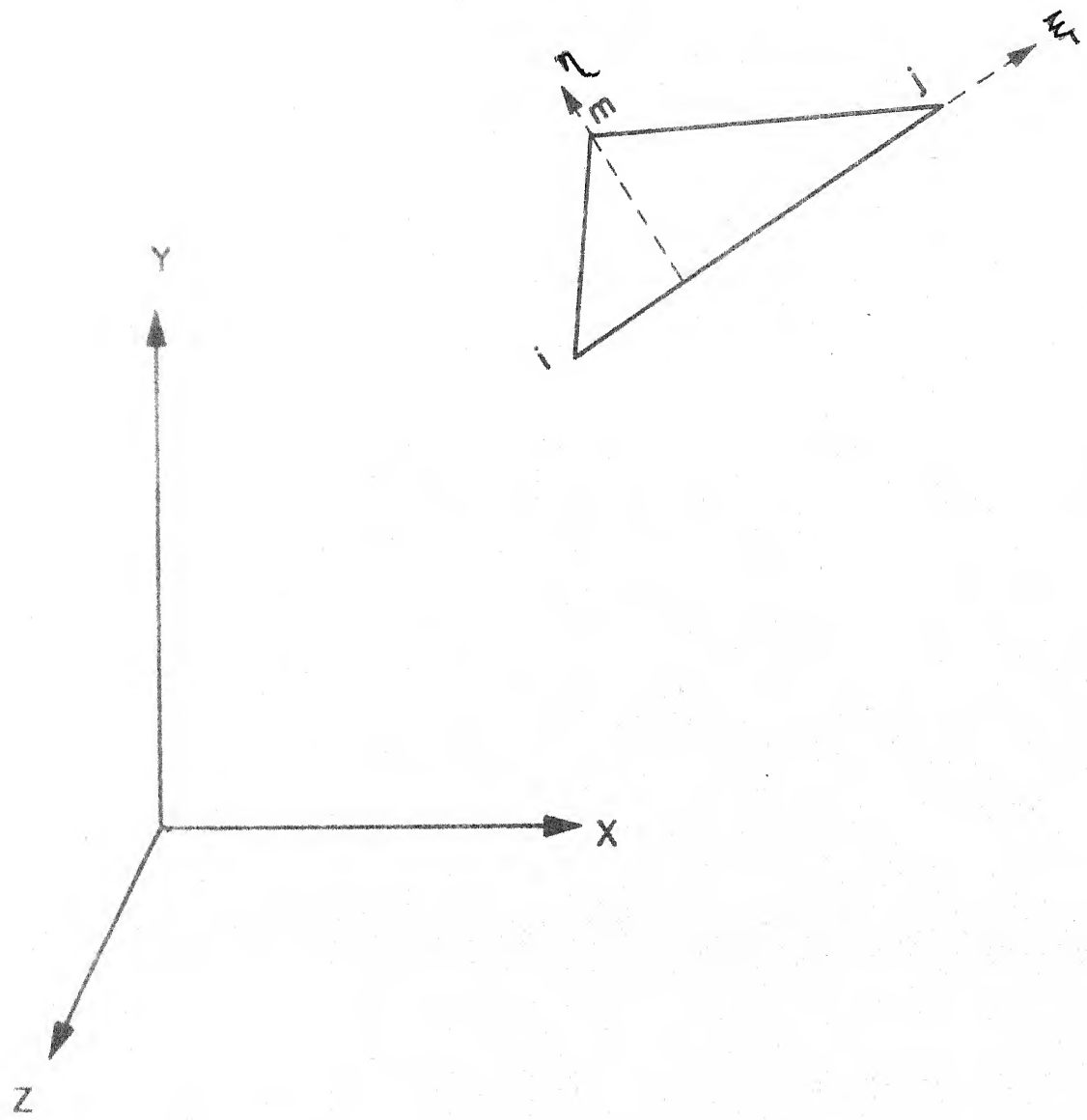

Fig. 4 Constant Stress Triangle

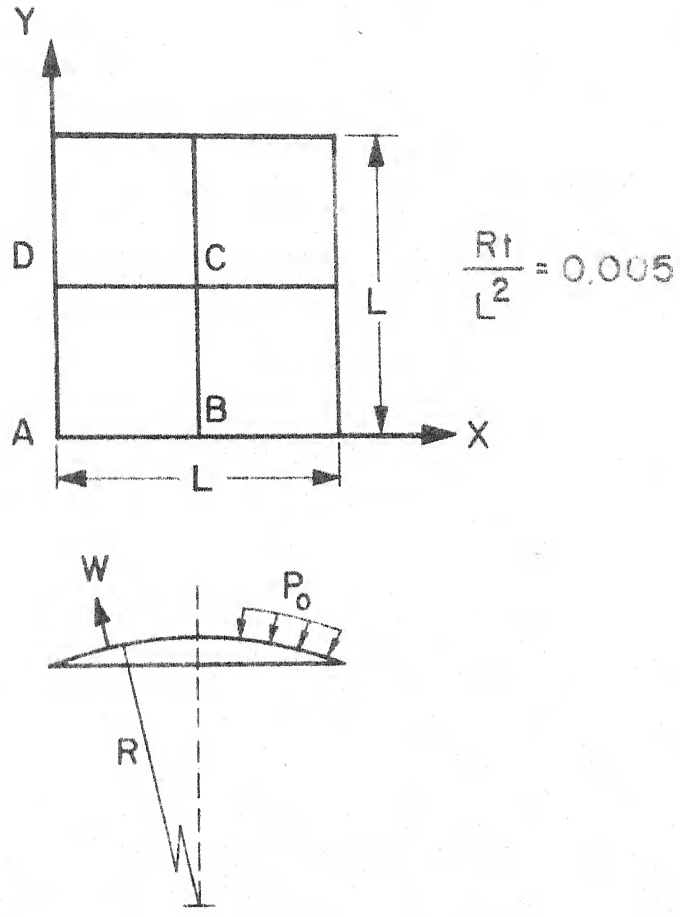

Fig.5 Spherical Cap

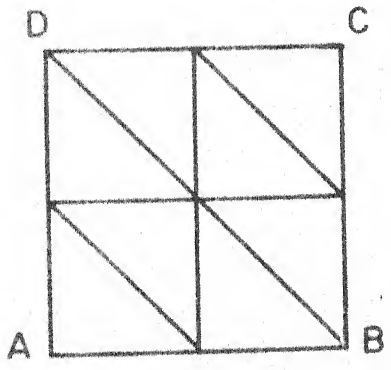

Fig.6 (a)

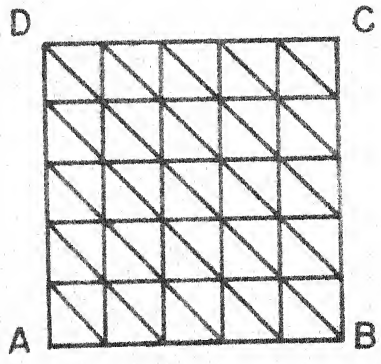

Fig.6(b)

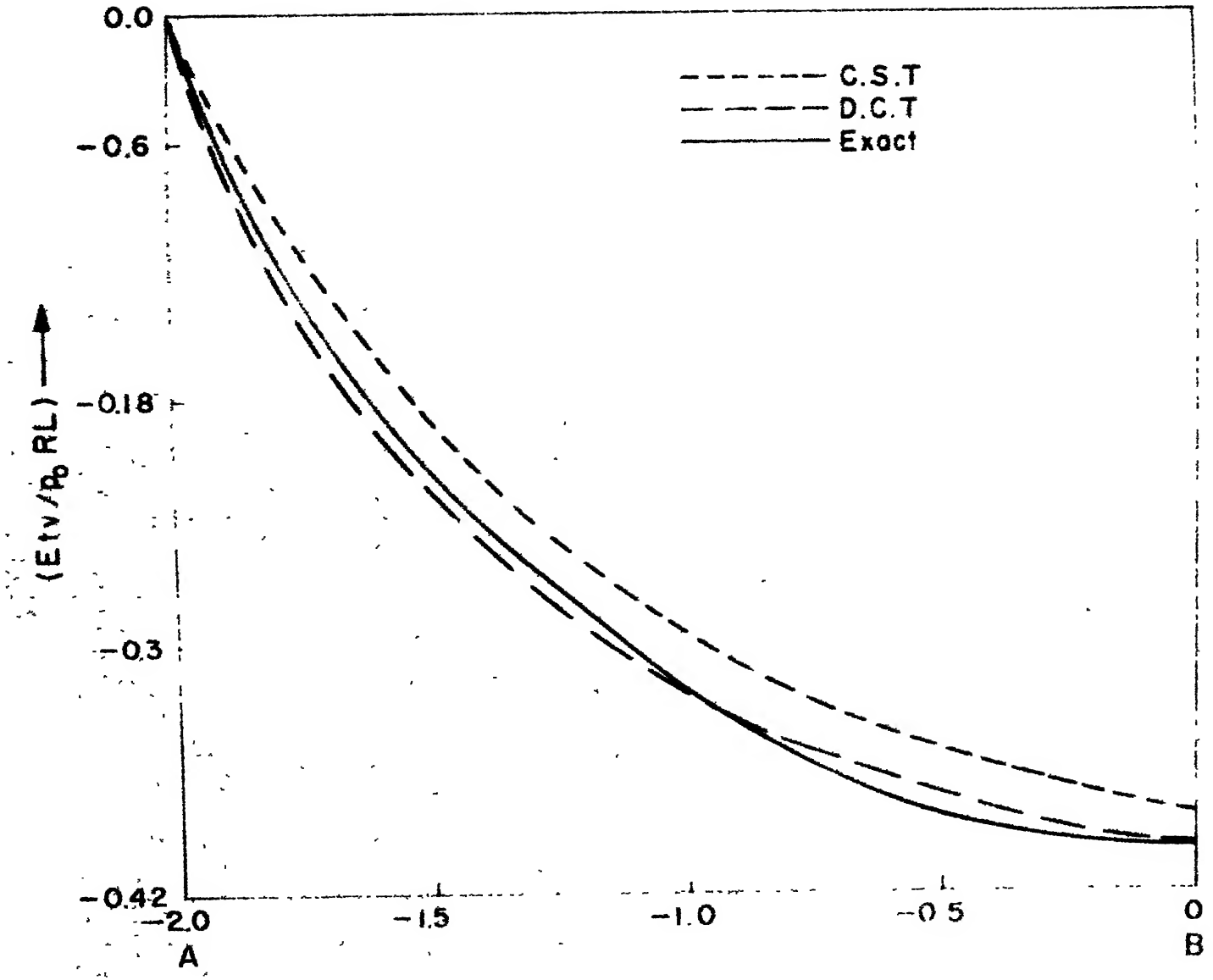

Fig. 7 Variation Of $(Etv/p_0 RL)$ Along Edge AB

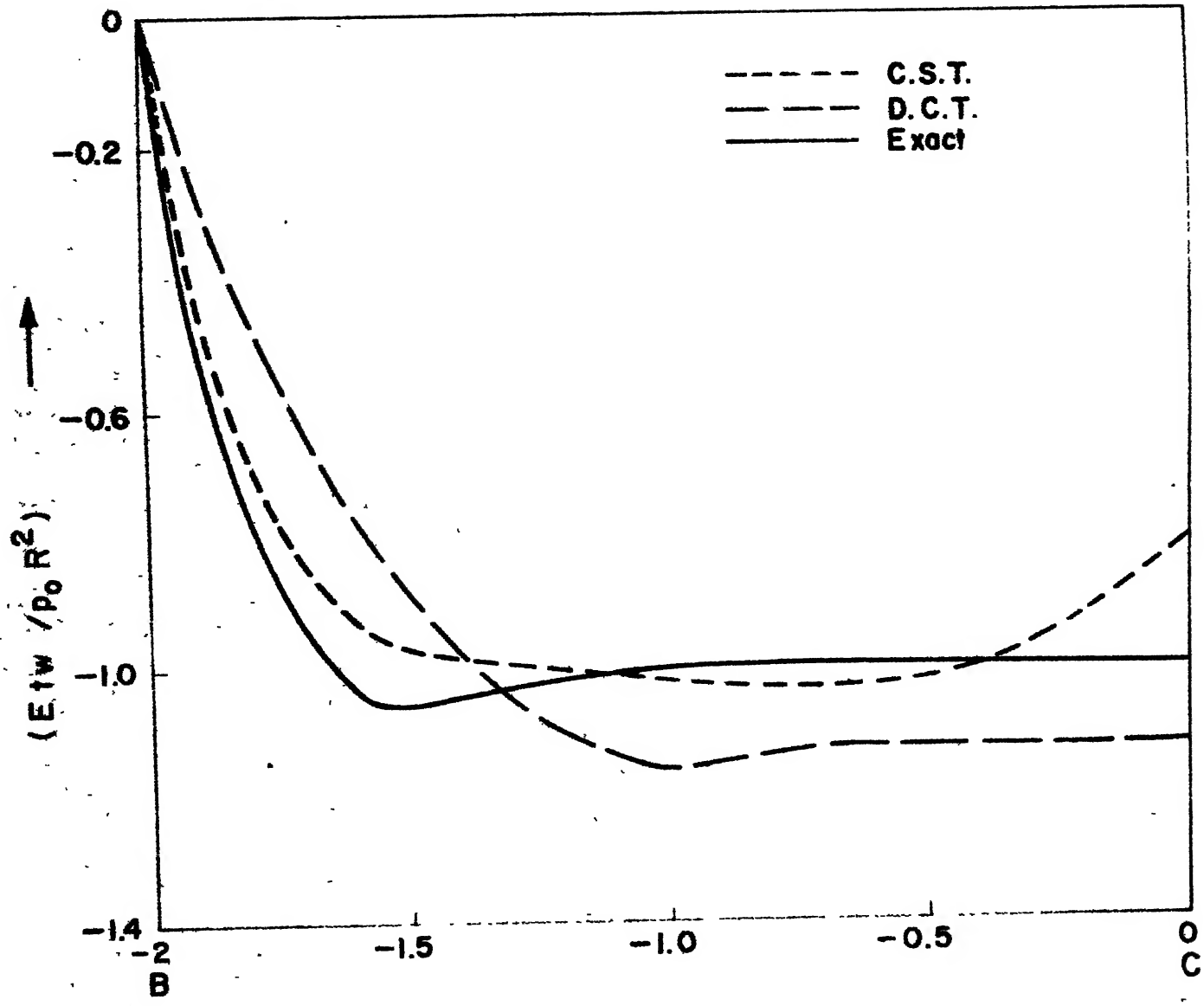

Fig. 8 Variation Of ($E t w / p_o R^2$) Along Edge BC

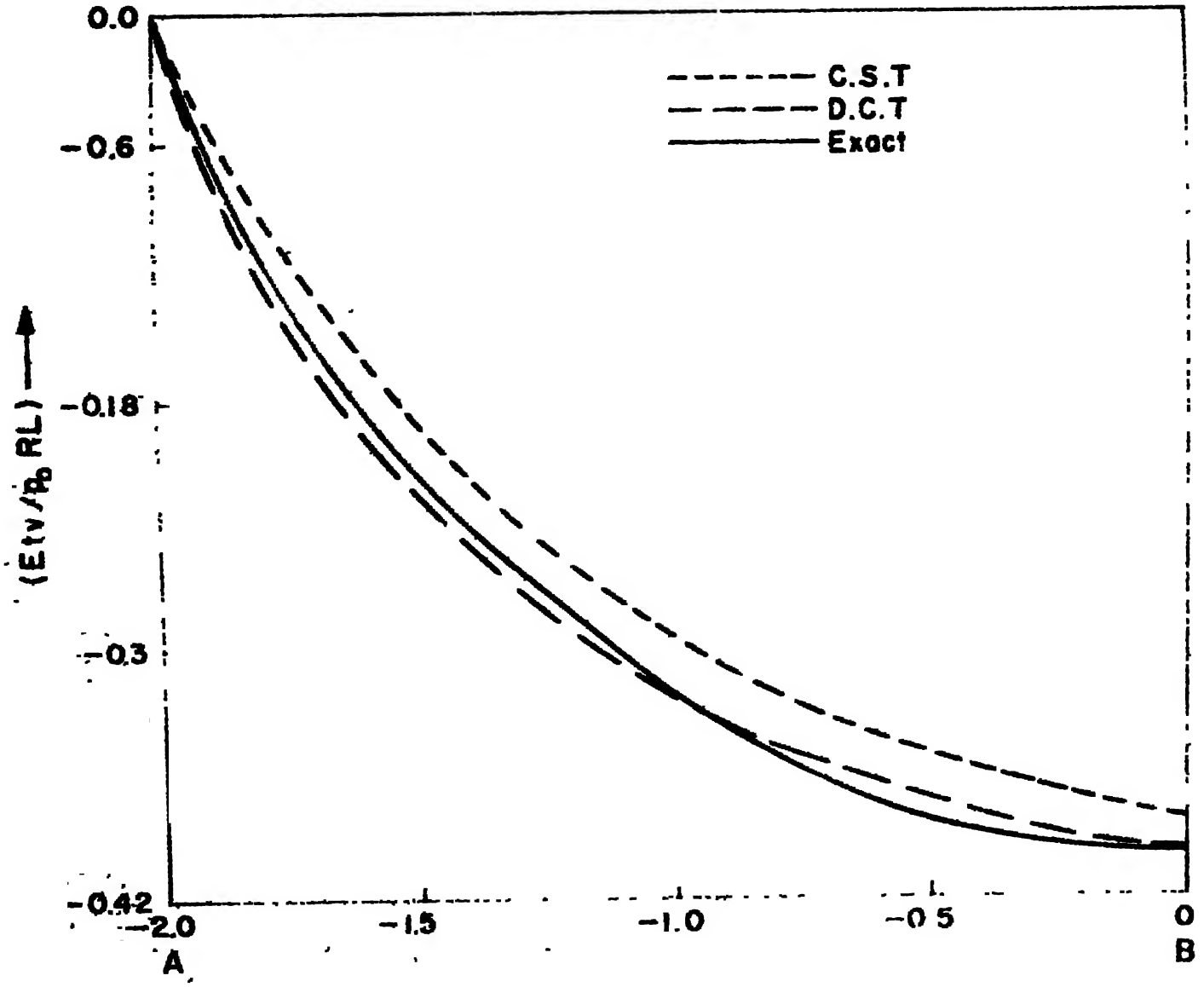

Fig. 7 Variation Of $(Etv/p_0 RL)$ Along Edge AB

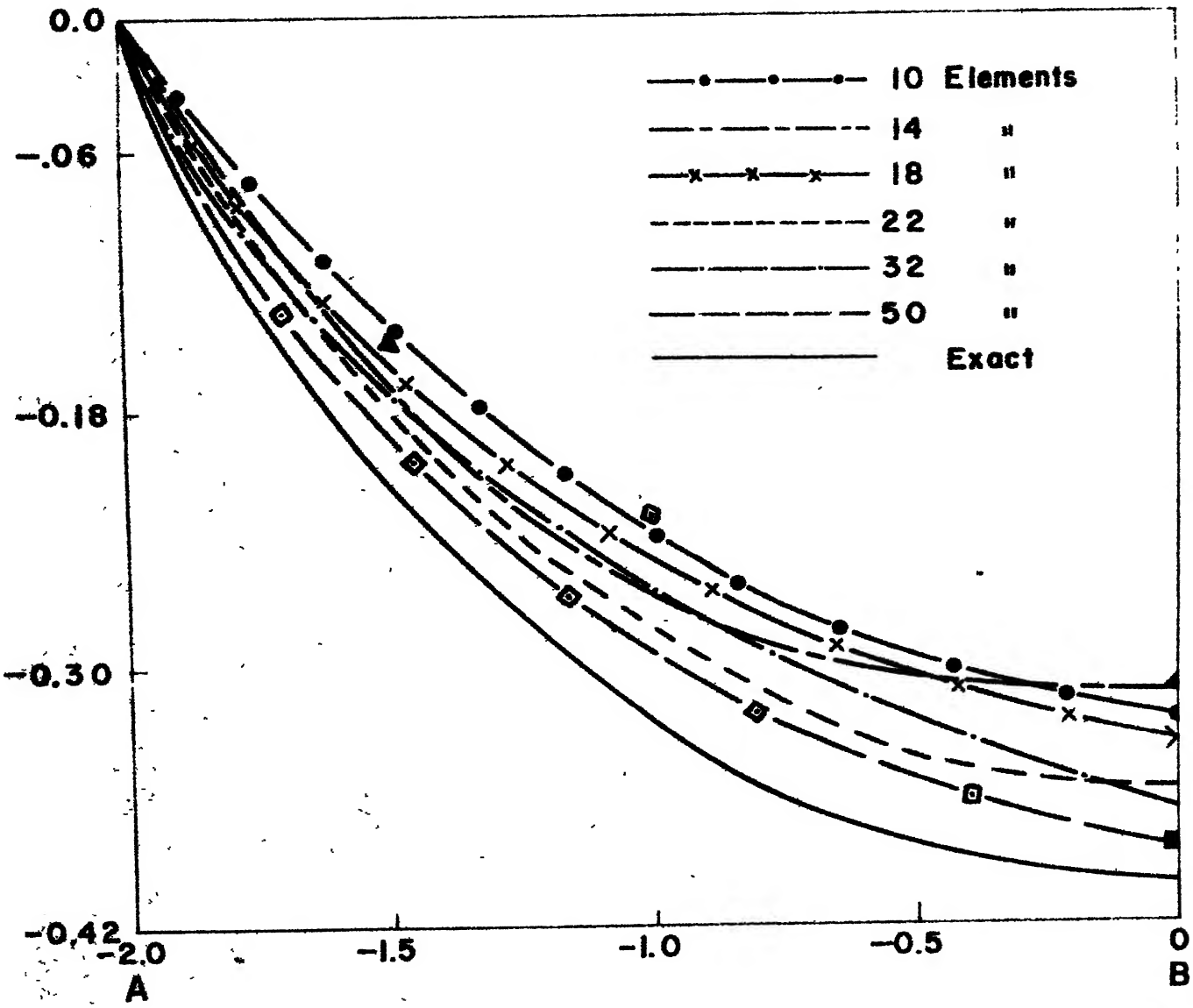

Fig. 10. Variation Of ($E t v / p_o RL$) Along Edge AB With Respect To Number Of Element

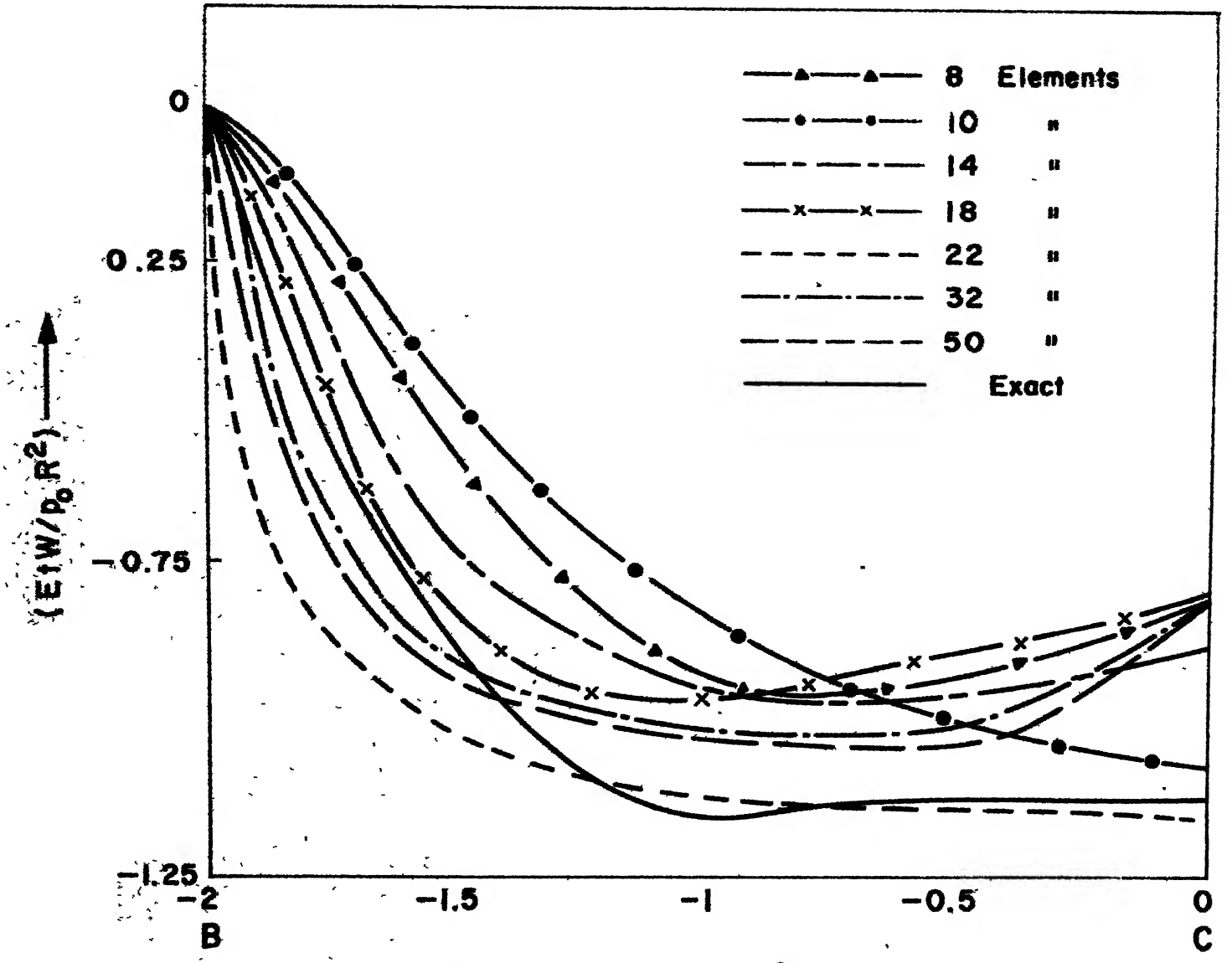

Fig.11 Variation Of ($Etw / p_o R^2$) Along Edge BC With Respect To Number Of Elements.

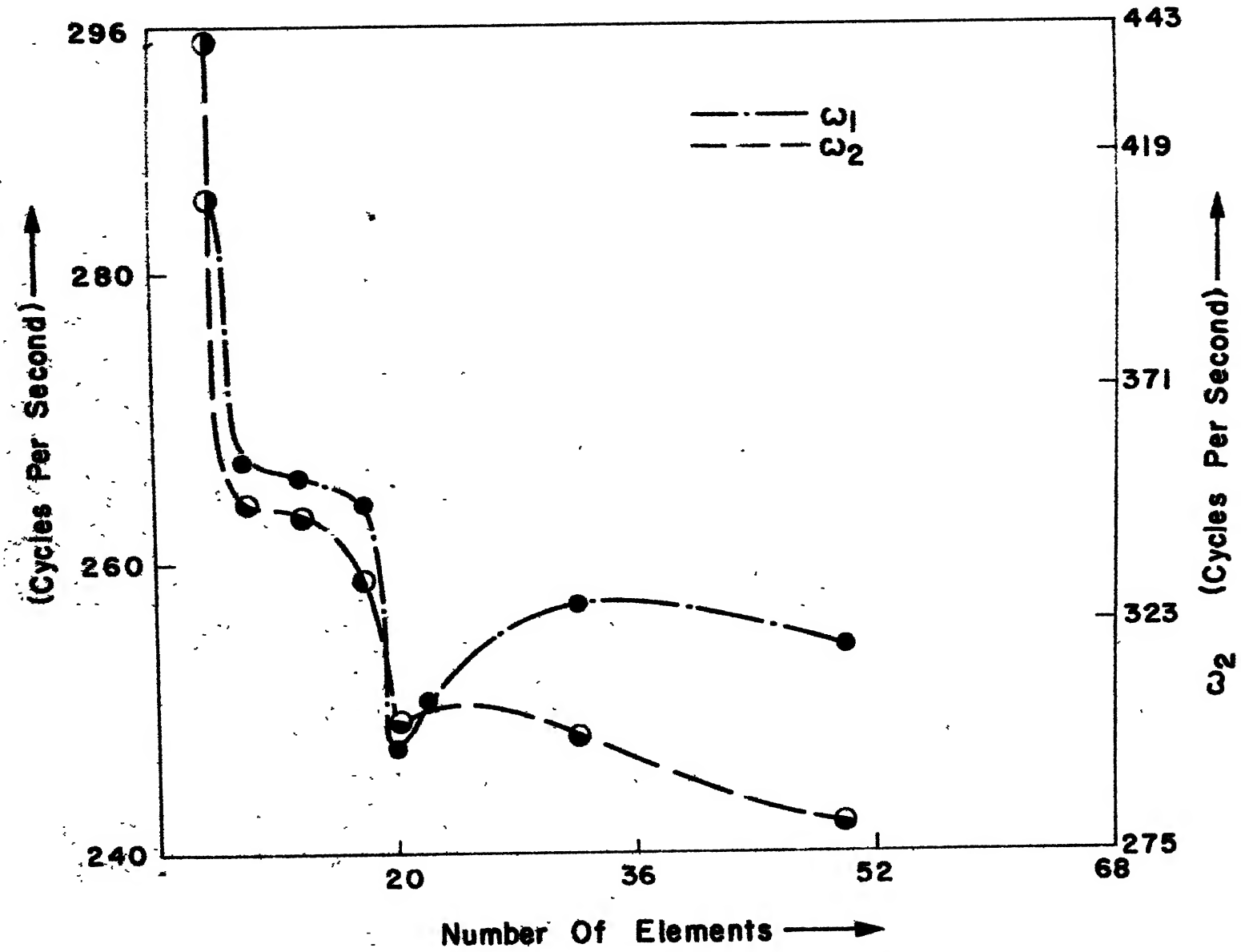

Fig.12 Variation Of Two Lowest Natural Frequency With Respect To Number Of Elements.

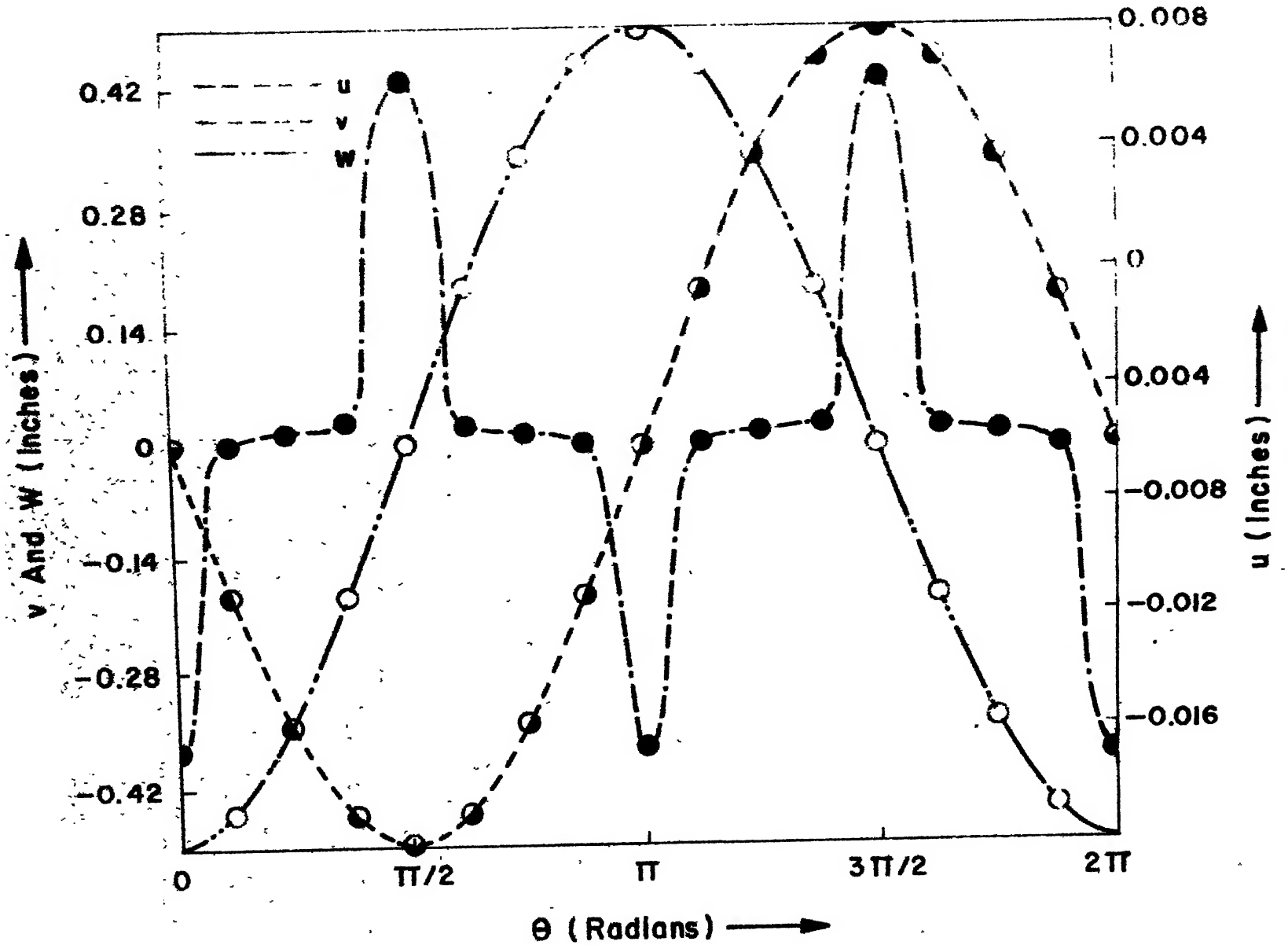

Fig.13 Plot Of u, v, w Vs θ Under Uniform Pressure (x = 12")

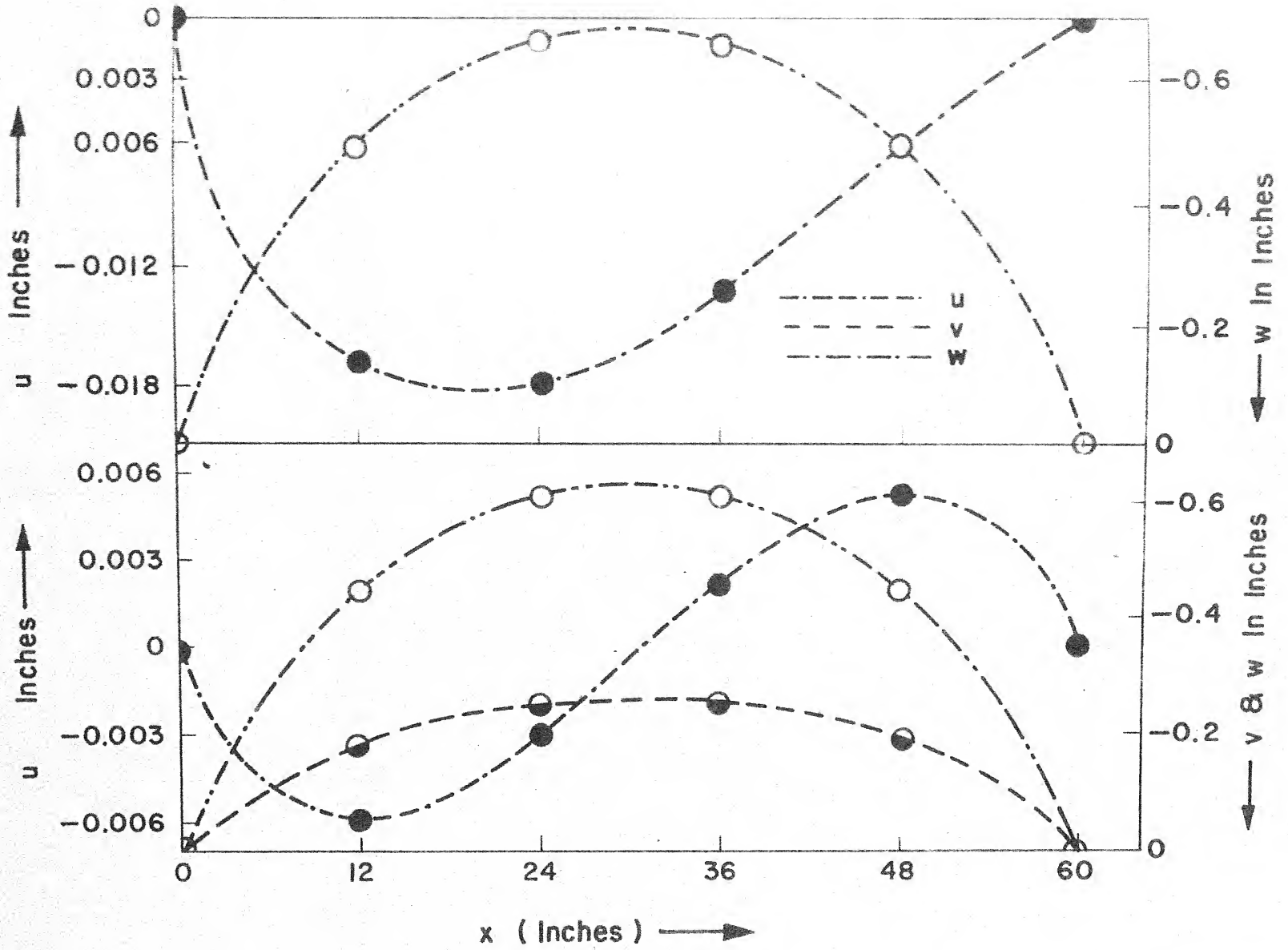

Fig. 14 Plot Of u, v, w Vs x Under Uniform Pressure ($\theta = 0^{\circ}, \theta = 22.5^{\circ}$)

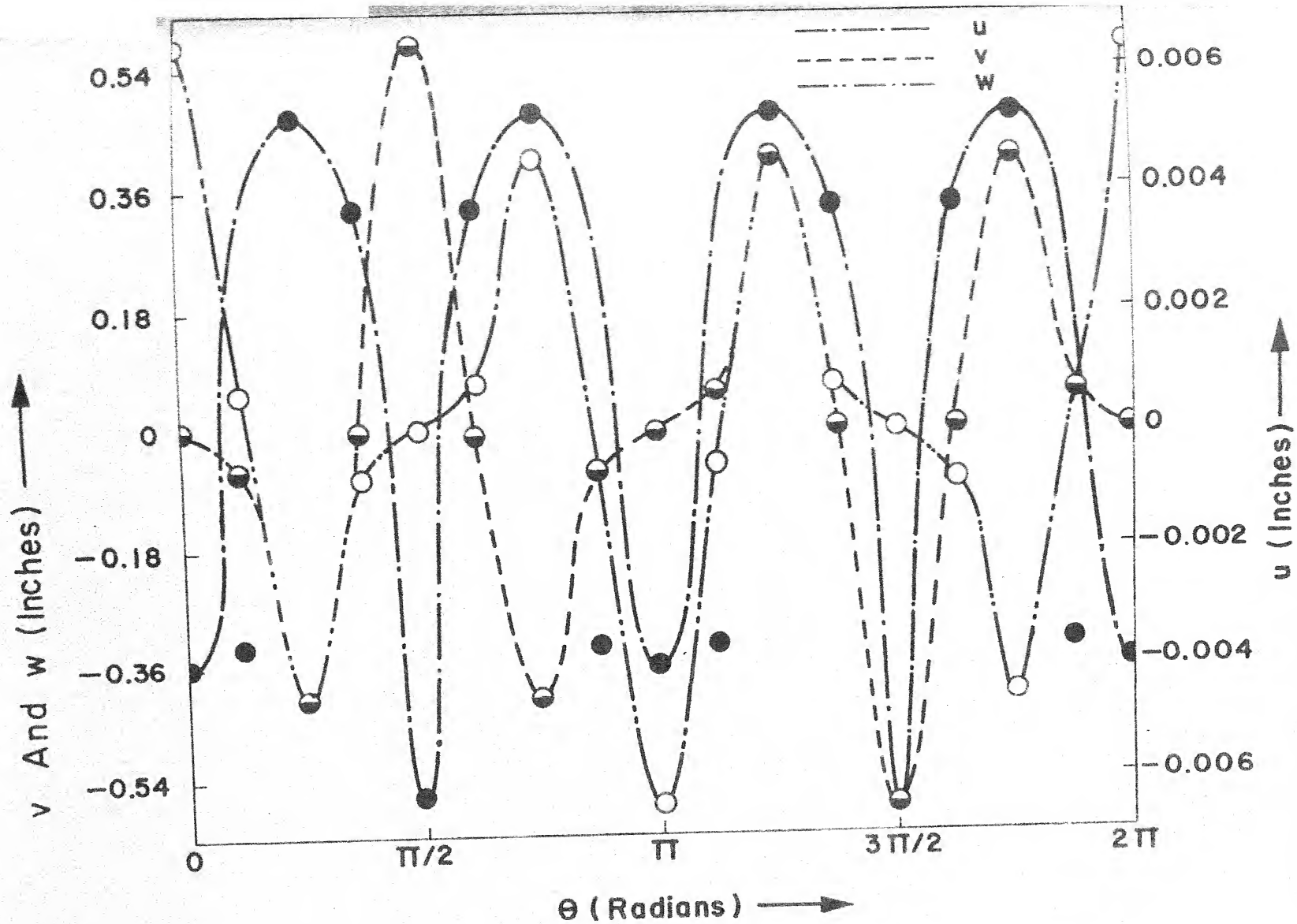

Fig. 15 Plot Of u, v, w Vs θ For Ist Mode (x = 12")

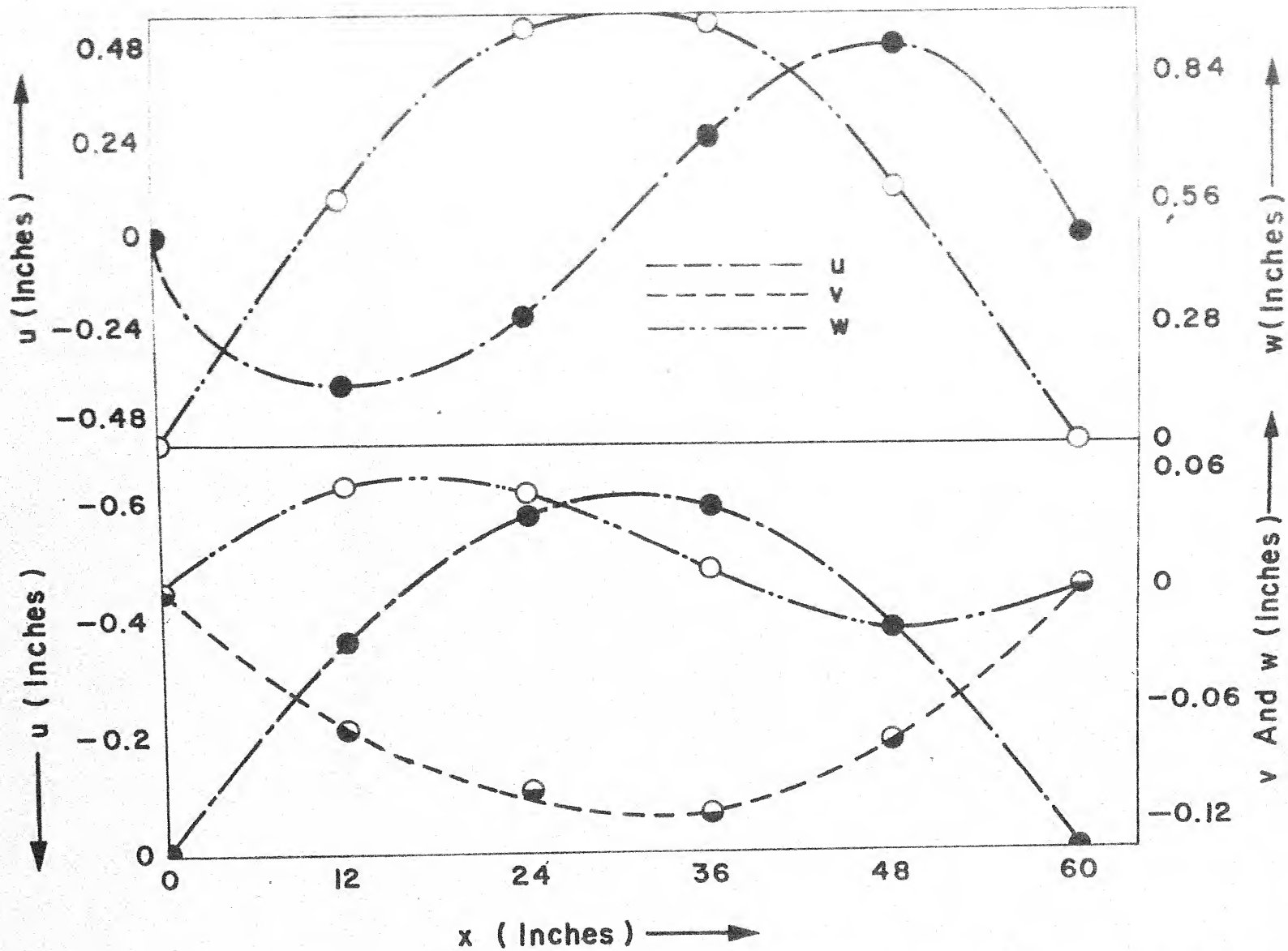

Fig.17 Plot Of u, v, w Vs Θ For Ist Mode ($\Theta = 0^\circ$, $\Theta = 22.5^\circ$)

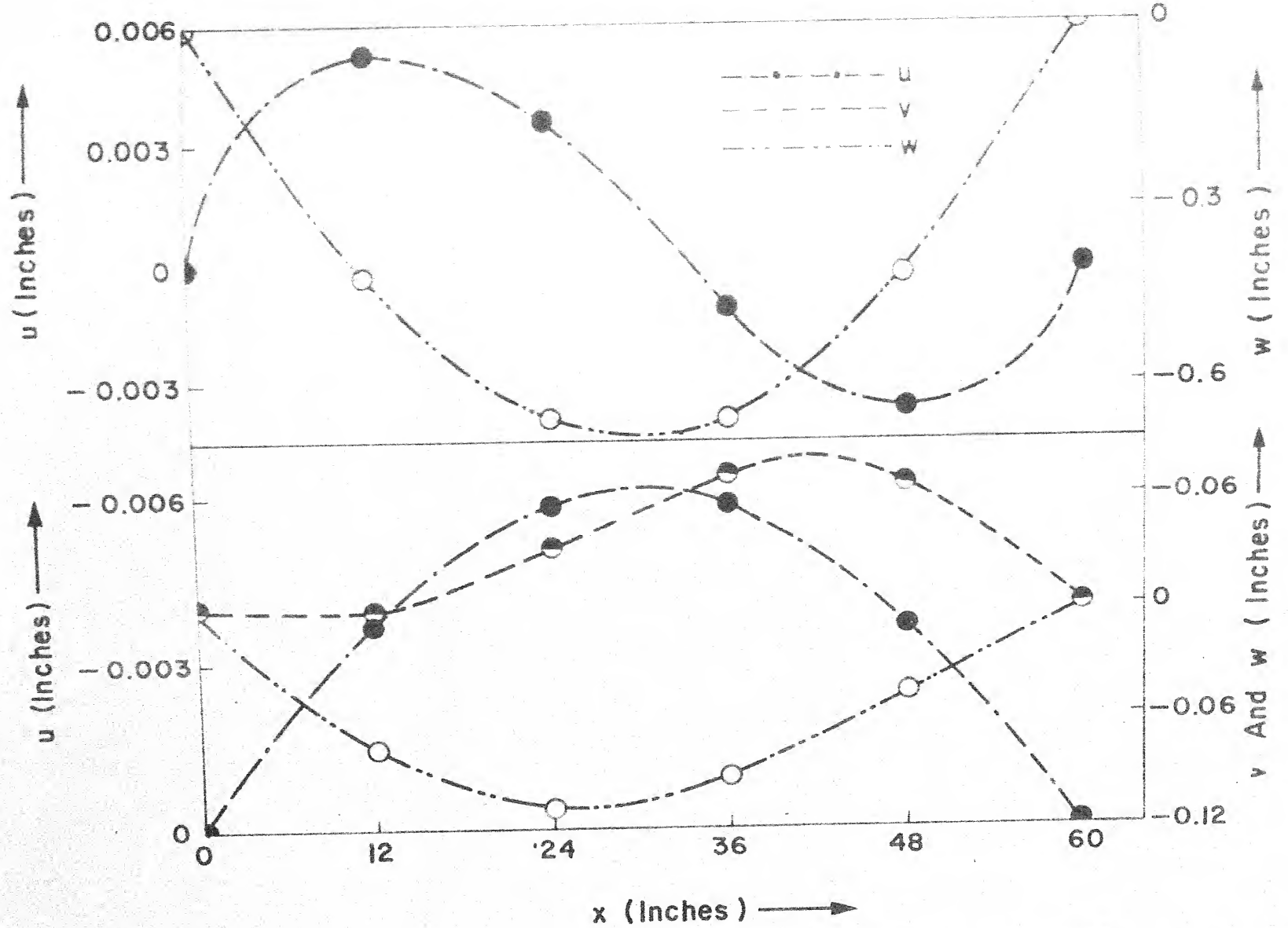

Fig. 18 Plot Of u, v, w Vs x For 1st Mode ($\theta = 45^\circ$, $\theta = 67.5^\circ$)

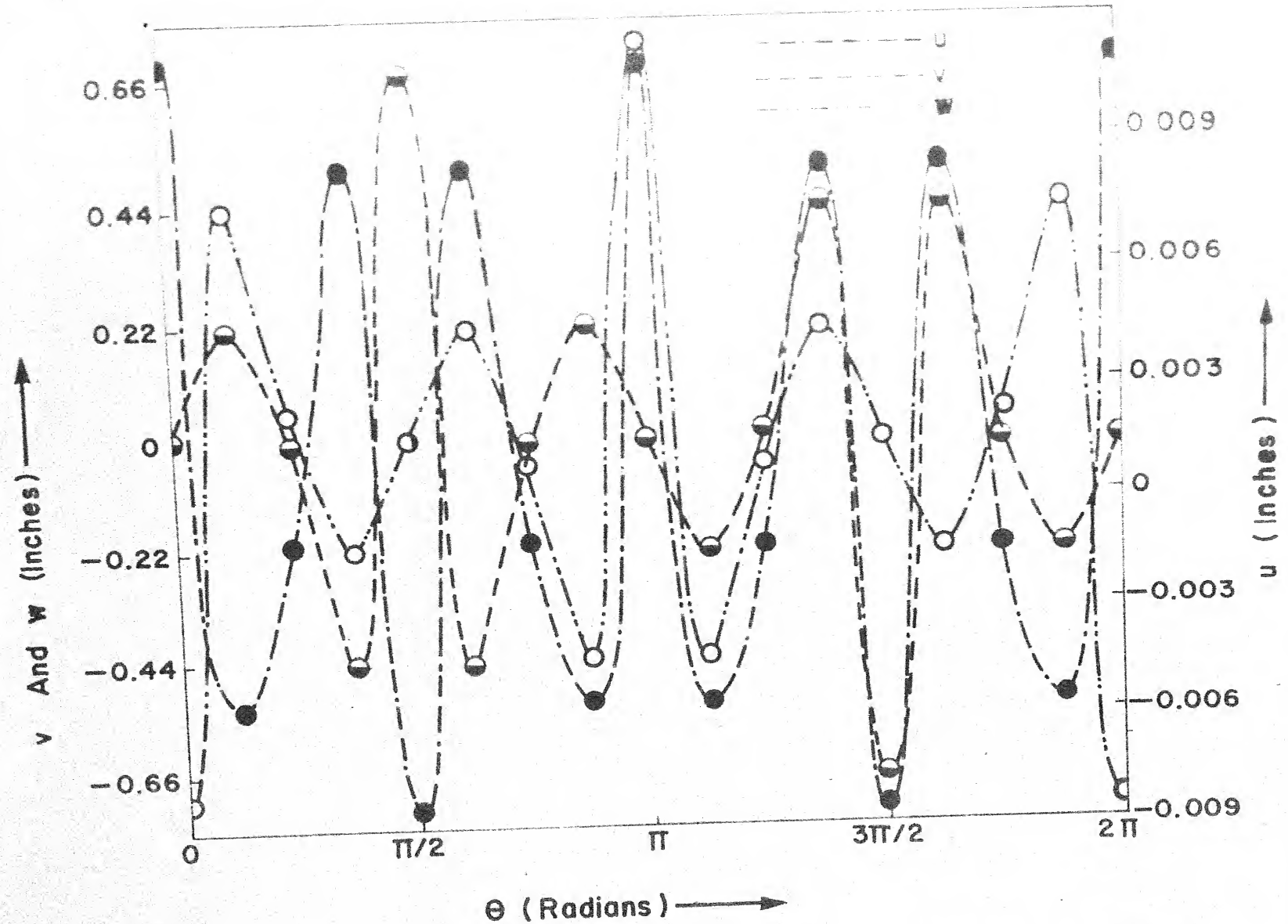

Fig. 19. Plot Of u, v, w Vs θ For The 2nd Mode (x = 12")

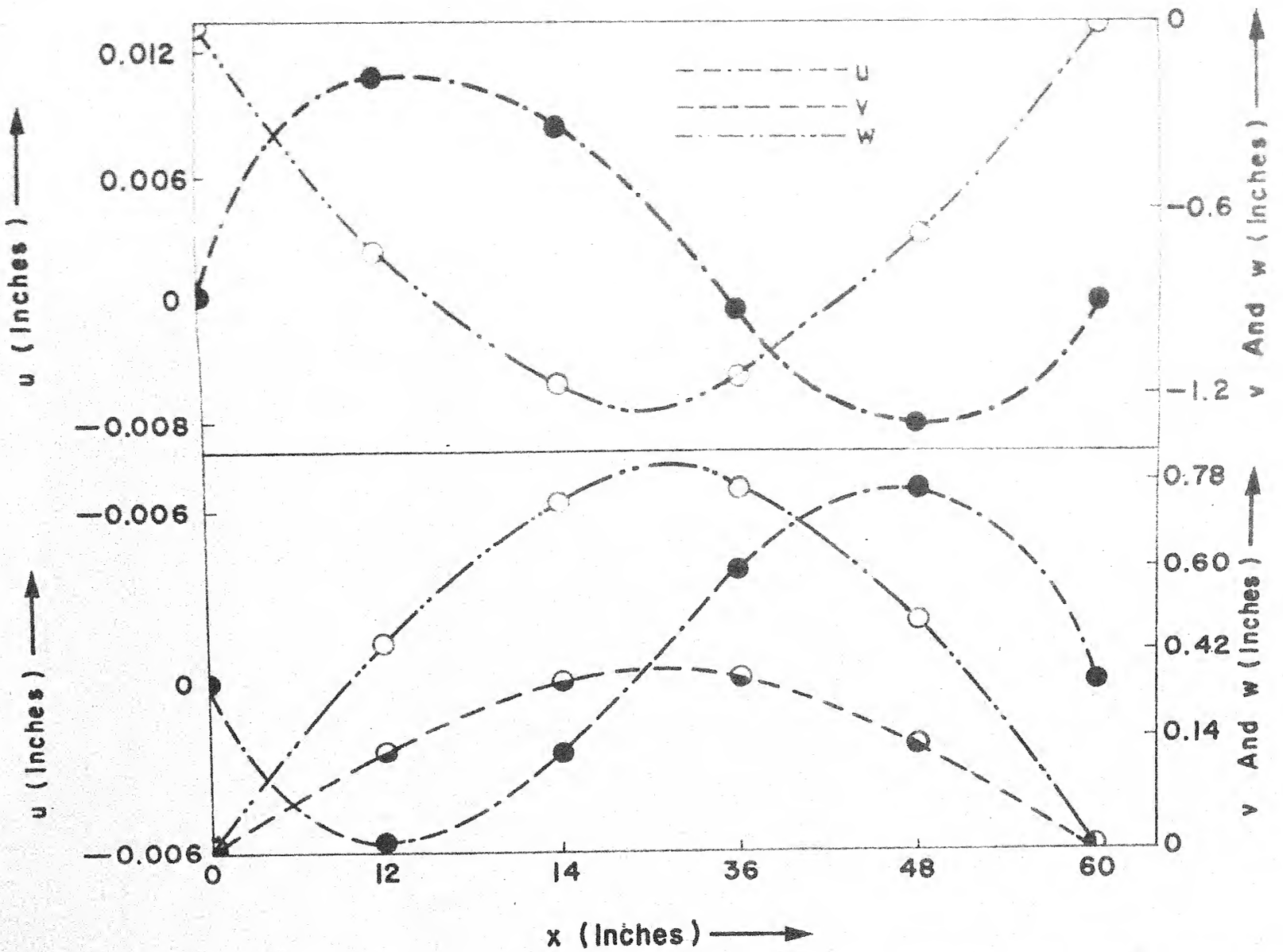

Fig. 20 Plot Of u, v, w Vs x For 2nd Mode ($\theta = 0°$, $\theta = 22.5°$)

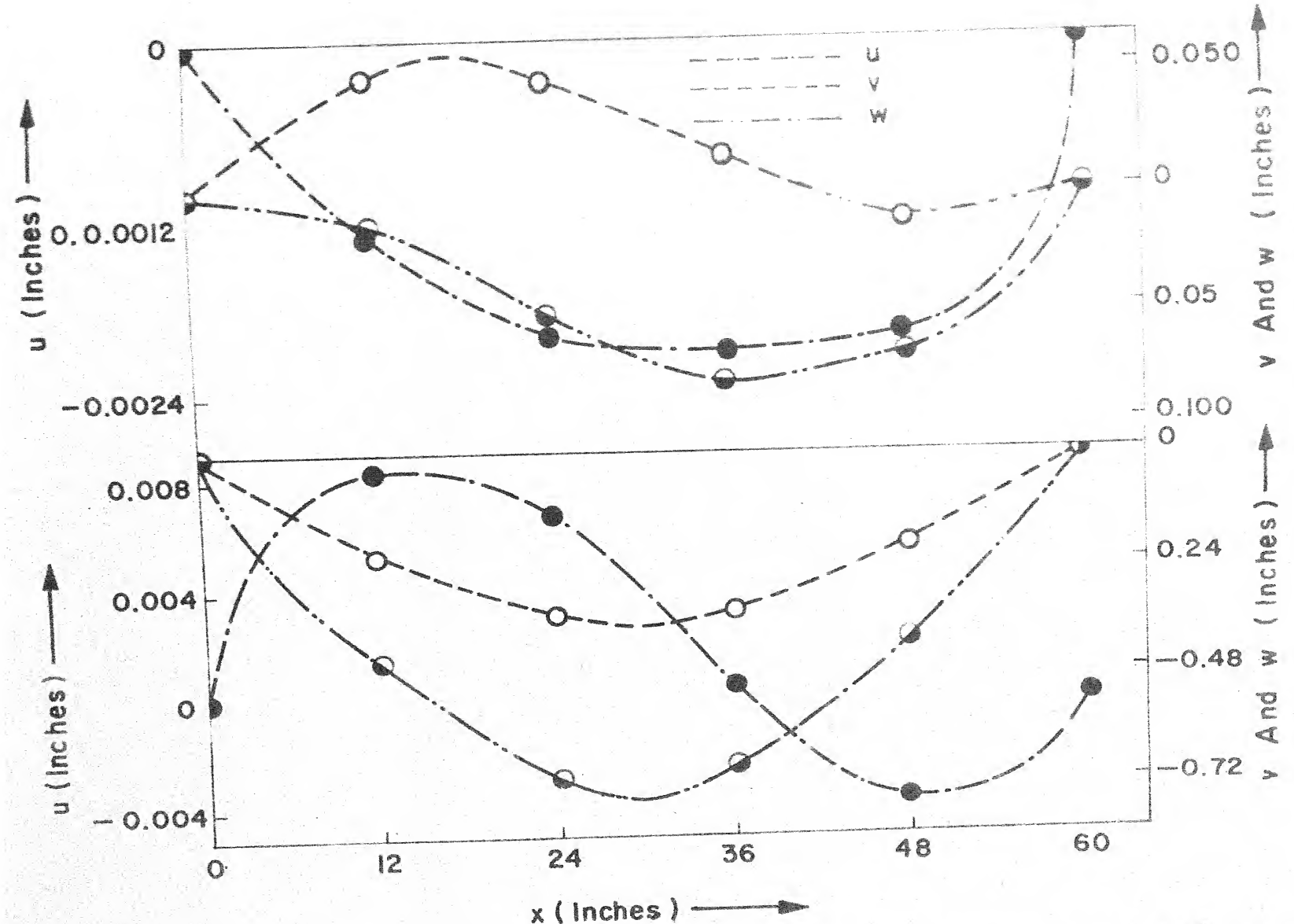

Fig. 21 Plot Of u, v, w Vs x For The 2nd Mode ($\theta = 45°$, $\theta = 67.5°$)

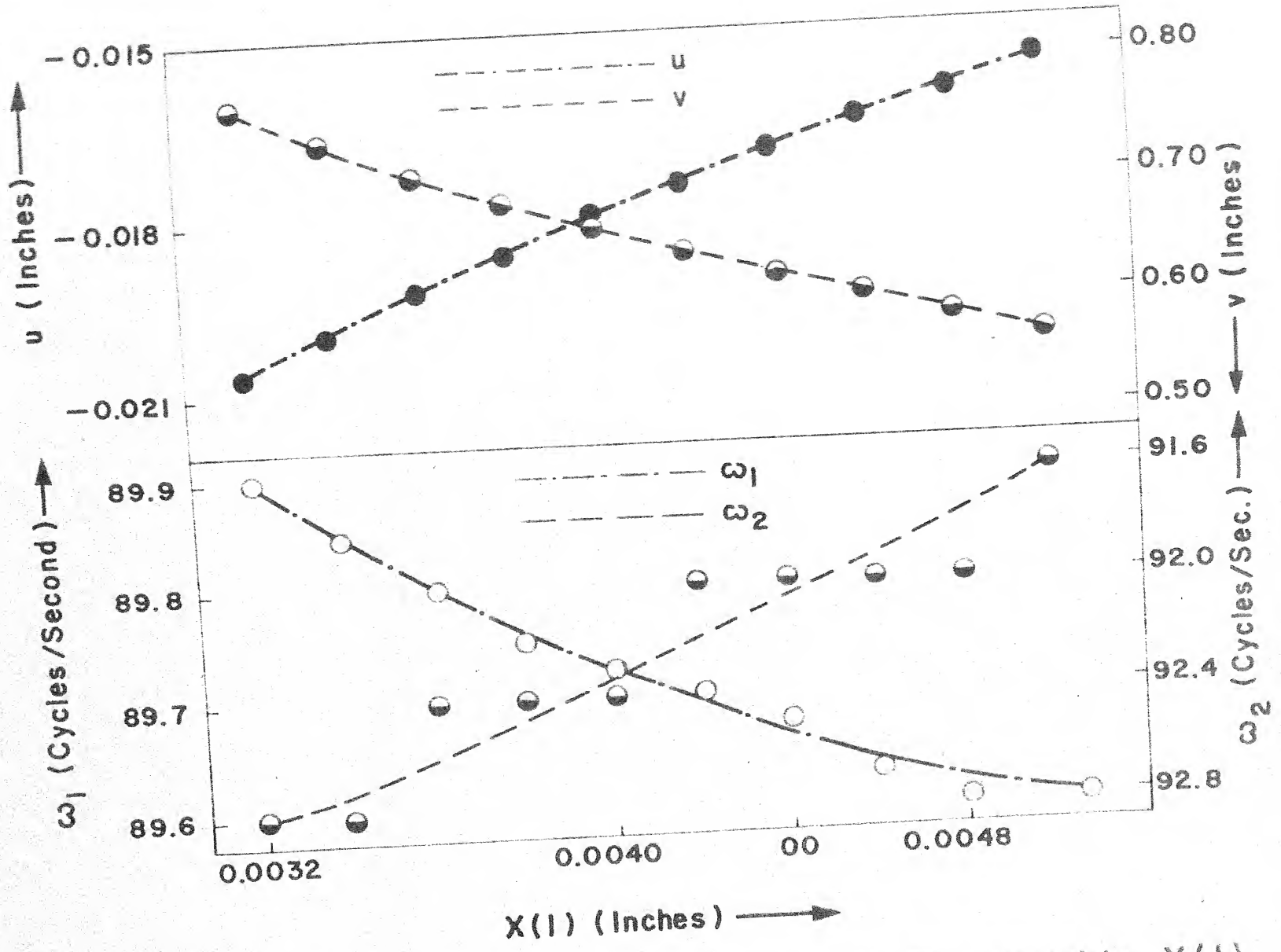

Fig. 22 Parametric Study With Respect To Variable X(1)

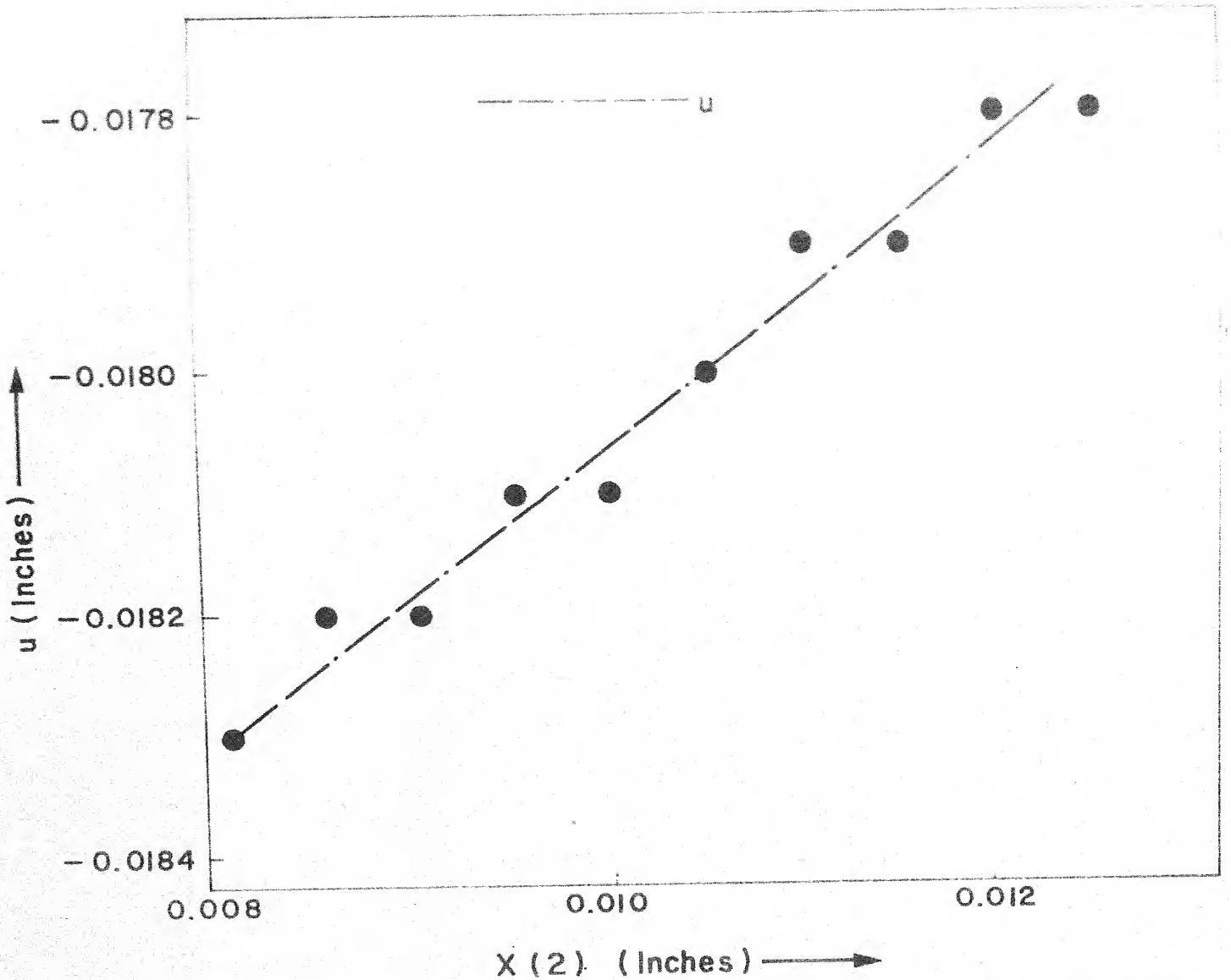

Fig. 23 Parametric Study With Respect [redacted] To Variable X(2)

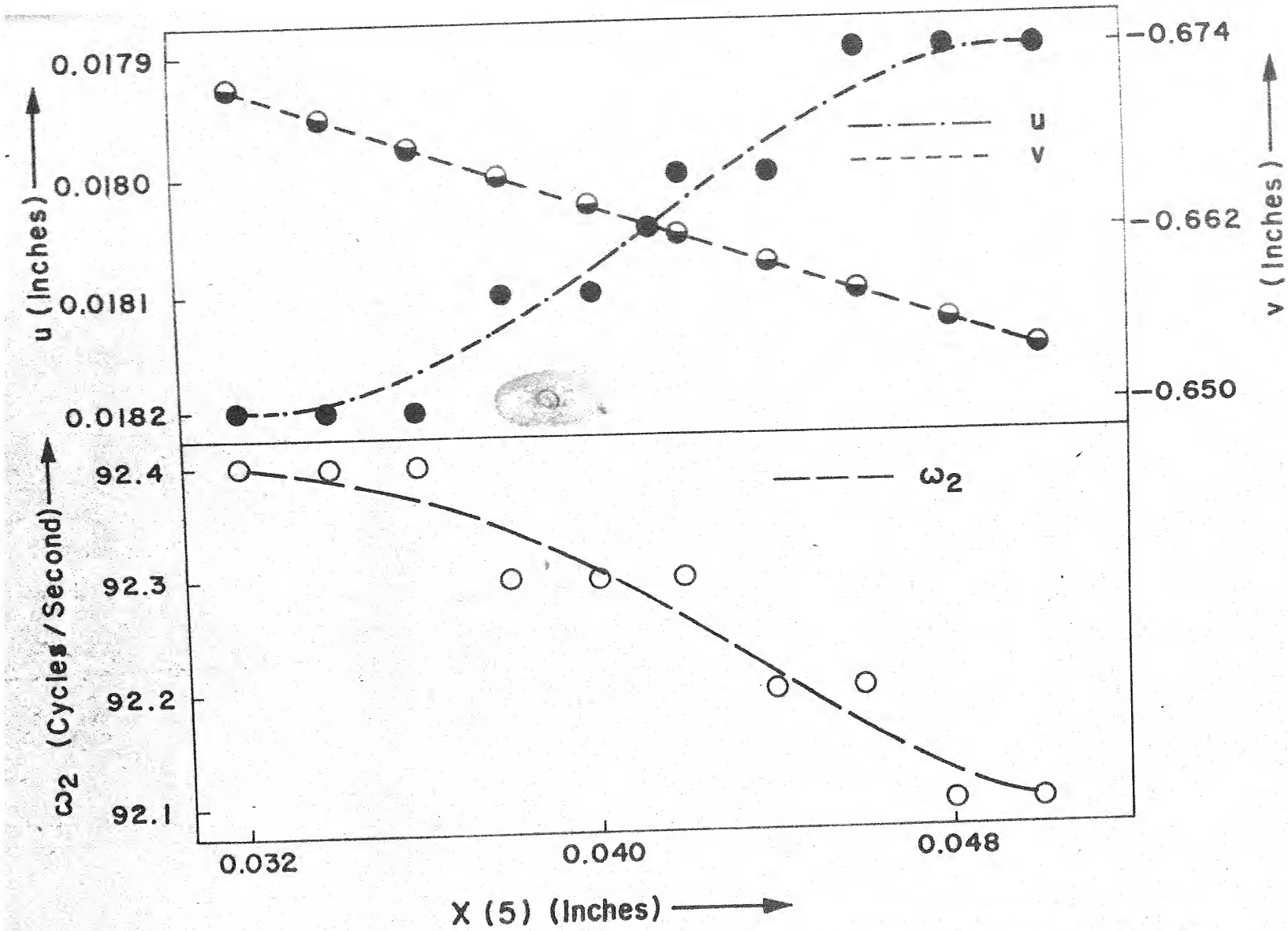

Fig. 24 Parametric Study With Respect To Variable X (5)

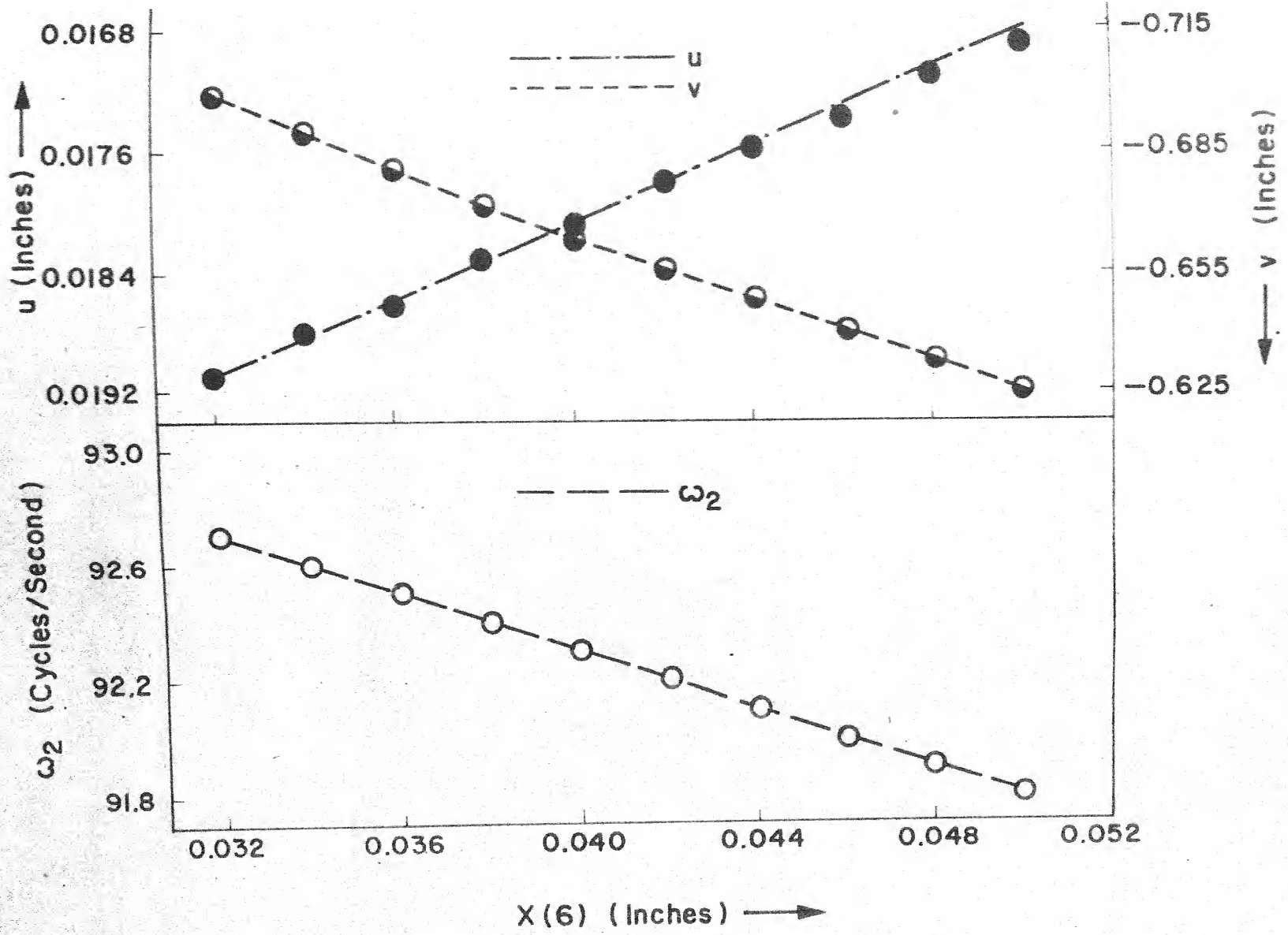

Fig. 25 Parametric Study With Respect To Variable X(6)

TABLE 1. COMPARATIVE STUDY

	D.O.F.*	ω_1 cycles/sec.	ω_2 cycles/sec.	Computer time
C.S.T.	75	254	280	51 sec.
D.C.T.	63	232	239	303 sec.

Changes in x y = -2	(EtV/p_oRL)		Changes in y x = 0	(EtW/p_oR^2)	
	C.S.T.	D.C.T.		C.S.T.	D.C.T.
-2.0	0	0	-2.0	0	0
-1.6	-0.1613	-	-1.6	-0.9044	-
-1.2	-0.2618	-	-1.2	-1.0091	-
-1.0	-	-0.3258	-1.0	-	-1.1609
-0.8	-0.3225	-	-0.8	-1.0286	-
-0.4	-0.3619	-	-0.4	-1.0200	-
0.0	-0.3850	-0.4080	0.0	-0.8004	-1.1301

* Degree of freedom.

TABLE 2. CONVERGENCE STUDY

Table 2.1 (EtV/p_oRL) variation along edge AB

No. elements / x-coordinate	10	14	18	22	32	50
-2.000	0	0	0	0	0	0
-1.600	-	-	-	-	-	-0.1613
-1.500	-	-0.1469	-	-0.1773	-0.1770	-
-1.333	-	-	-0.1939	-	-	-
-1.200	-	-	-	-	-	-0.2618
-1.000	-0.2392	-	-	-	-0.2796	-
-0.800	-	-	-	-	-	-0.3225
-0.666	-	-	-0.2913	-	-	-
-0.500	-	-0.2621	-	-0.3423	-0.3360	-
-0.4000	-	-	-	-	-	-0.3619
-0.009	-0.3249	-0.3109	-0.3362	-0.3584	-0.3671	-0.3850

Table 2.2 (EtW/p_oR^2) variation along edge BC

No. elements / y-coordinate	10	14	18	22	31	50
-2.000	0.0000	0.0000	0.0000	0.0000	0.0000	0.0000
-1.600	-	-	-	-	-	-0.9044
-1.500	-	-0.7276	-	-1.1032	0.9138	-
-1.333	-	-	-0.9307	-	-	-
-1.200	-	-	-	-	-	-1.0091
-1.000	-0.8255	-	-	-	-1.0190	-
-0.800	-	-	-	-	-	-1.0286
-0.666	-	-	-1.0142	-	-	-
-0.500	-	-1.0989	-	-1.1458	-1.0225	-
-0.400	-	-	-	-	-	-1.0200
-0.000	-1.0793	-0.8754	-0.8113	-1.1643	-0.8081	-0.8004

Table 2.3 ω_1 and ω_2 variation

No. elements	10	14	18	22	32	50
1	266	266	264	250	257	254
2	345	345	331	305	297	280

TABLE 3. PARAMETRIC STUDY*

Design variable	Percentage change in design variable	$ux10^{-2}$ inches	$vx10^{-1}$ inches	$wx10^{-1}$ inches	ω_1 cycles/sec.	ω_2 cycles/sec.
X(1)	0	-1.81	-6.64	-6.64	89.7	92.3
	-20	-2.06	-7.70	-7.70	89.6	91.6
	-15	-1.99	-7.40	-7.40	89.7	91.8
	-10	-1.92	-7.13	-7.13	89.7	92.0
	- 5	-1.86	-6.88	-6.88	89.7	92.2
	+ 5	-1.75	-6.42	-6.42	89.8	92.4
	+10	-1.70	-6.21	-6.21	89.8	92.5
	+15	-1.65	-6.02	-6.02	89.8	92.7
	+20	-1.61	-5.03	-5.03	89.8	92.8
	+25	-1.56	-5.66	-5.66	89.9	92.8
X(5)	0	-1.81	-6.64	-6.64	89.7	92.3
	-20	-1.82	-6.72	-6.72	89.7	92.4
	-15	-1.82	-6.70	-6.70	89.7	92.4
	-10	-1.82	-6.68	-6.68	89.7	92.4
	- 5	-1.81	-6.66	-6.66	89.7	92.3
	+ 5	-1.80	-6.62	-6.62	89.7	92.3
	+10	-1.80	-6.60	-6.60	89.7	92.2
	+15	-1.79	-6.58	-6.58	89.7	92.2
	+20	-1.79	-6.56	-6.56	89.7	92.1
	+25	-1.79	-6.54	-6.54	89.7	92.1
X(6)	0	-1.81	-6.64	-6.64	89.7	92.3
	-20	-1.91	-6.99	-6.99	89.7	92.7
	-15	-1.88	-6.90	-6.90	89.7	92.6
	-10	-1.86	-6.81	-6.81	89.7	92.5
	- 5	-1.83	-6.72	-6.72	89.7	92.4
	+ 5	-1.78	-6.56	-6.56	89.7	92.2
	+10	-1.76	-6.48	-6.48	89.7	92.1
	+15	-1.74	-6.40	-6.40	89.7	92.0
	+20	-1.71	-6.32	-6.32	89.7	91.9
	+25	-1.69	-6.25	-6.25	89.7	91.8

* X(2), X(3) and X(4) do not cause appreciable changes in the value of u, v, w, ω_1 and ω_2.

TABLE 4. OPTIMISATION RESULTS

Table 4.1. For first starting point

	Initial value	Final value	Percentage change
X(1)	0.5	0.3656	21.0
X(2)	0.1	0.9743	2.7
X(3)	0.5	0.4903	1.4
$F(\overline{X})$	0.5355	0.4291	20.0
g(12)	-0.231	-0.099	57.0
g(13)	-0.231	-0.098	57.0
g(14)	-0.231	-0.098	57.0

Table 4.2. For 2nd starting point

	Initial value	Final value	Percentage change
X(1)	0.008	0.005917	26.0
X(2)	0.008	0.007903	1.2
X(3)	0.050	0.048760	2.4
$F(\overline{X})$	0.011503	0.009268	18.5
g(12)	-0.231	-0.093	59.0
g(13)	-0.231	-0.097	57.0
g(14)	-0.231	-0.095	58.0

REFERENCES

(1) Bard, Y.: "On numerical instability of Davidon like methods", Math. Comp., July 1968, p. 665.

(2) Bathe, K.S. and Wilson, E.L.: "Large eigenvalue problems in dynamic analysis", EM6, Dec. 1972, p. 1471.

(3) Broyden, C.G.: "Quasi Newton method and their application to function minimisation", Math. Comp. 21, 1967, p. 368.

(4) Coxter, H.S.M.: "Golden Section", Scripta Mathematica, 1954.

(5) Davidon, W.C., "Variable metric method for minimisation", AFC research and development report, ANL 5996, 1959.

(6) Fletcher, R. and Reeves, C.M.: "Function minimisation by conjugate direction", Computer Journal, 1964, p. 149.

(7) Fletcher, R. and Powell, M.J.D.: "A rapidly convergent descent method for minimisation", Computer Journal, 1964, p. 163.

(8) Fox, R.L.: "Optimisation method for engineering design", Addison Wesley Publication, 1971.

(9) Fox, R.L. and Kapoor, M.P., "A minimisation method for solution of eigenvalue problem in structural dynamics", 2nd Conference on matrix method in structural mechanics, W.P.A.F.B., Ohio, Oct. 1968.

(10) Gerard and Papirino: "Minimum weight design of stiffened cylinders for launch vehicles", NASA CR-533, March 1964.

(11) Joycee, M.B. and Mitchell, L.A.: "Panel shape for least weight design of stiffened cylinders in pure pending", Council for scientific and industrial research, Australia Div. of Aero. S.M. 106, Dec. 1947.

(12) Kicher: "Structural synthesis of integrally stiffened cylinders", Journal of Spacecraft and Rockets, Vol. 5, Jan. 1968.

(13) Legget, D.M.A. and Hopkins, H.G.: "Sandwich panels and cylinders under compressive end loads", Aeronautical Research Council, RM 2202, Aug. 1949.

(14) Novozilov, V.V.: "The theory of thin shell", 2nd edition, Section 7a, Noordoff, 1964.

(15) Olsen, M.D., Lindberg, G.M. and Cowper, U.R.: "A shallow shell finite element of triangular shape", Inter. J. of Solids and Structures, 1970, Vol. 6, p. 1133.

(16) Olsen, M.D. and Lindberg, G.N.:"Dynamic analysis of shallow shells with a doubly curved triangular finite elements", J. of Sound and Vibrations, 1971, Vol. 19, p. 1299.

(17) Powell, M.J.D.: "An iterative method for finding stationary values of a function of several variables", Computer J., 1962, pp 147-151.

(18) Przemieniecki, J.S.: "Theory of matrix structural analysis", McGraw Hill, New York, 1968.

(19) Ralston, A.: "A first course in numerical analysis", McGraw Hill,

(20) Rao, S.S.: "Automated design of aircraft wings to satisfy strength, stability, frequency, flutter requirements", Ph.D. Thesis, Case Western Reserve Univ., Jan. 1972.

(21) Schmit, Kicher and Morrow: "Structural synthesis capabilities for integrally stiffened waffle plates", AIAA J. Vol. 1, No. 12, Dec. 1963.

(22) Wittrick, W.A.: "A theoretical analysis of the efficiency of sandwich construction under compressive end loads", Aeronautical research council RM 2016, April 1945.

(23) Ungbahakorn, V. and Simitses, G.J.L "Minimum weight design of stiffened cylinders under axial compression", AIAA J., June 1975, Vol. 13, No. 6.

(24) Zienkiechwich, O.C.: "The finite element method in engineering sciences", 2nd ed., McGraw Hill, New York, 1971.

APPENDIX A

The 40 x 40 matrix [T]: See Fig. 3 for the definition of symbols a, b, c, θ and ρ

$$[T] = \begin{bmatrix} S_1 & 0 & 0 \\ 0 & S_1 & 0 \\ 0 & 0 & S_2 \\ S_3 & 0 & 0 \\ 0 & S_3 & 0 \\ 0 & 0 & S_4 \\ S_5 & 0 & 0 \\ 0 & S_5 & 0 \\ 0 & 0 & S_6 \\ S_7 & 0 & 0 \\ 0 & S_7 & 0 \\ 0 & 0 & S_8 \end{bmatrix}$$

$$[S_1] = \begin{bmatrix} 1 & -b & 0 & b^2 & 0 & 0 & 0 & -b^3 & 0 & 0 & 0 \\ 0 & 1 & 0 & -2b & 0 & 0 & 0 & 3b^2 & 0 & 0 & 0 \\ 0 & 0 & 1 & 0 & -2b & -b & 0 & 0 & b^2 & 0 & 0 \end{bmatrix}$$

$$[S_2] = [S_{2a} \quad S_{2b}]$$

$$[S_{2a}] = \begin{bmatrix} 1 & -b & 0 & b^2 & 0 & 0 & -b^3 & 0 & 0 & 0 \\ 0 & 1 & 0 & -2b & 0 & 0 & 3b^2 & 0 & 0 & 0 \\ 0 & 0 & 1 & 0 & -b & 0 & 0 & b^2 & 0 & 0 \\ -0 & 0 & 0 & 2 & 0 & 0 & -6b & 0 & 0 & 0 \\ 0 & 0 & 0 & 0 & 1 & 0 & 0 & -2b & 0 & 0 \\ 0 & 0 & 0 & 0 & 0 & 2 & 0 & 0 & -2b & 0 \end{bmatrix}$$

$$[S_{2b}] = \begin{bmatrix} b^4 & 0 & 0 & 0 & 0 & -b^5 & 0 & 0 & 0 & 0 \\ -4b^3 & 0 & 0 & 0 & 0 & 5b^4 & 0 & 0 & 0 & 0 \\ 0 & -b^3 & 0 & 0 & 0 & 0 & 0 & 0 & 0 & 0 \\ 12b^2 & 0 & 0 & 0 & 0 & -20b^3 & 0 & 0 & 0 & 0 \\ 0 & 3b^2 & 0 & 0 & 0 & 0 & 0 & 0 & 0 & 0 \\ 0 & 0 & 2b^2 & 0 & 0 & 0 & -2b^3 & 0 & 0 & 0 \end{bmatrix} 0$$

$$[S_3] = \begin{bmatrix} 1 & a & 0 & a^2 & 0 & 0 & a^3 & 0 & 0 & 0 \\ 0 & 1 & 0 & 2a & 0 & 0 & 3a^2 & 0 & 0 & 0 \\ 0 & 0 & 1 & 0 & a & 0 & 0 & a^2 & 0 & 0 \end{bmatrix}$$

$$[S_4] = \begin{bmatrix} S_{4a} & S_{4b} \end{bmatrix}$$

$$[S_{4a}] = \begin{bmatrix} 1 & a & 0 & a^2 & 0 & 0 & a^3 & 0 & 0 & 0 \\ 0 & 1 & 0 & 2a & 0 & 0 & 3a^2 & 0 & 0 & 0 \\ 0 & 0 & 1 & 0 & a & 0 & 0 & a^2 & 0 & 0 \\ 0 & 0 & 0 & 2 & 0 & 0 & 6a & 0 & 0 & 0 \\ 0 & 0 & 0 & 0 & 1 & 0 & 0 & 2a & 0 & 0 \\ 0 & 0 & 0 & 0 & 0 & 2 & 0 & 0 & 2a & 0 \end{bmatrix}$$

$$[S_{4b}] = \begin{bmatrix} a^4 & 0 & 0 & 0 & 0 & a^5 & 0 & 0 & 0 & 0 \\ 4a^3 & 0 & 0 & 0 & 0 & 5a^4 & 0 & 0 & 0 & 0 \\ 0 & a^3 & 0 & 0 & 0 & 0 & 0 & 0 & 0 & 0 \\ 12a & 0 & 0 & 0 & 0 & 20a^3 & 0 & 0 & 0 & 0 \\ 0 & 3a^2 & 0 & 0 & 0 & 0 & 0 & 0 & 0 & 0 \\ 0 & 0 & 2a^2 & 0 & 0 & 0 & 2a^3 & 0 & 0 & 0 \end{bmatrix}$$

$$[S_5] = \begin{bmatrix} 1 & 0 & c & 0 & 0 & c^2 & 0 & 0 & 0 & c^3 \\ 0 & 1 & 0 & 0 & c & 0 & 0 & 0 & c^2 & 0 \\ 0 & 0 & 1 & 0 & 0 & 2c & 0 & 0 & 0 & 3c^2 \end{bmatrix}$$

$$[S_6] = [S_{6a} \quad S_{6b}]$$

$$[S_{6a}] = \begin{bmatrix} 1 & 0 & c & 0 & 0 & c^2 & 0 & 0 & 0 & c^3 \\ 0 & 1 & 0 & 0 & c & 0 & 0 & 0 & c^2 & 0 \\ 0 & 0 & 1 & 0 & 0 & 2c & 0 & 0 & 0 & 3c^2 \\ 0 & 0 & 0 & 2 & 0 & 0 & 0 & 2c & 0 & 0 \\ 0 & 0 & 0 & 0 & 1 & 0 & 0 & 0 & 2c & 0 \\ 0 & 0 & 0 & 0 & 0 & 2 & 0 & 0 & 0 & 6c \end{bmatrix}$$

$$[S_{6b}] = \begin{bmatrix} 0 & 0 & 0 & 0 & c^4 & 0 & 0 & 0 & 0 & c^5 \\ 0 & 0 & 0 & c^3 & 0 & 0 & 0 & 0 & c^4 & 0 \\ 0 & 0 & 0 & 0 & 4c^3 & 0 & 0 & 0 & 0 & 5c^4 \\ 0 & 0 & 2c^2 & 0 & 0 & 0 & 0 & 2c^3 & 0 & 0 \\ 0 & 0 & 0 & 3c^2 & 0 & 0 & 0 & 0 & 4c^3 & 0 \\ 0 & 0 & 0 & 0 & 12c^2 & 0 & 0 & 0 & 0 & 2c^3 \end{bmatrix}$$

$$[S_7] = \left[1, \frac{a-b}{}, \frac{c}{3}, \frac{(a-b)^2}{9}, \frac{(a-b)c}{9}, \frac{c^2}{9}, \frac{(a-b)^3}{27}, \frac{(a-b)^2 c}{27}, \frac{(a-b)c^2}{27}, \frac{c^3}{27} \right]$$

$$[S_8 = [S_{8a} \quad S_{8b}]$$

$$[S_{8a}] = \begin{bmatrix} 0 & 0 & 0 & 0 & 0 & 0 & 0 & 0 & 0 & 0 & 0 & 0 & 0 & 0 \\ 0 & 0 & 0 & 0 & 0 & 0 & 0 & 0 & 0 & 0 & 0 & 0 & 0 & 0 \end{bmatrix}$$

$$[S_{8b}] = \begin{bmatrix} (5a^4c, & 3a^2c^3 - 2a^4c, & -2ac^4 + 3a^3c^2, \\ c^5 - 4a^2c^3, & 5ac^4) & \\ (5b^4c, & 3b^2c^3 - 2b^4c, & 2bc^4 - 5b^3c^2, \\ c^5 - 4b^2c^3, & -5bc^4) & \end{bmatrix}$$

ELEMENTS OF STIFFNESS MATRIX:

See Eq. (24) for the definition of the symbols m_i, n_i, p_i, q_i, r_i and s_i.

$$
\begin{aligned}
k_{ij} = {} & m_i m_j F(m_i+m_j-2,\ n_i+n_j) + q_i q_j F(p_i+p_j,\ q_i+q_j-2) \\
& + \tfrac{1}{2}(1-\nu)\left[n_i n_j F(m_i+m_j,\ n_i+n_j-2) + p_i p_j F(p_i+p_j-2,\right. \\
& \left. q_i+q_j) \right] + \left[\tfrac{1}{2}(1-\nu) n_j p_i + \nu m_j q_i) \right] F(m_j+p_i-1, \\
& n_j+q_i+1) + \left[\tfrac{1}{2}(1-\nu) n_i p_j + \nu m_i q_j) \right] F(m_i+p_j-1,\ n_i+q-1) \\
& - (\rho_{\xi\xi} + \nu \rho_{\eta\eta}) \left[m_i F(m_i+r_j-1,\ n_i+s_j) + m_j F(m_j+r_i-1, \right. \\
& \left. n_j+s_i) \right] - (\rho_{\xi\xi} + \nu \rho_{\eta\eta}) \left[q_i F(p_i+r_j,\ q_i+s_j-1) + \right. \\
& \left. q_j F(p_j+r_i,\ q_j+s_i-1) \right] - (1-\nu) \rho_{\xi\eta} \left[n_i F(m_i+r_j, \right. \\
& \left. n_i+s_j-1) + n_j F(m_j+r_i,\ n_j+s_i-1) + p_i F(p_i+r_j-1, \right. \\
& \left. q_i+s_j) + p_j F(p_j+r_i-1,\ q_j+s_i) \right] + \left[\rho_{\xi\xi}^2 + \rho_{\eta\eta}^2 + \right. \\
& \left. 2\nu \rho_{\xi\xi} \rho_{\eta\eta} + 2(1-\nu^2) \rho_{\xi\eta}^2 \right] F(r_i+r_j,\ s_i+s_i) \\
& + \frac{t^2}{12} r_i r_j (r_i-1)(r_j-1) F(r_i+r_j-4,\ s_i+s_j) \\
& + s_i s_j (s_i-1)(s_j-1) F(r_i+r_j,\ s_i+s_j-4) + \frac{t^2}{12} \\
& \left[2(1-\nu) r_i r_j s_i s_j + \nu\ r_i s_j (r_i-1)(s_j-1) + \nu r_j s_i (r_j-1) \right. \\
& \left. (s_i-1) \right] F(r_i+r_j-2,\ s_i+s_j-2)
\end{aligned}
$$

where $F(m,n) = c^{n+1}\left[a^{m+1} - (-b)^{m+1}\right]\frac{m!\ n!}{(m+n+2)!}$

for i & j = 1,2,...,40.

ROTATION MATRIX $[R]$:

$$[R] = \begin{bmatrix} R_1 & 0 & 0 & 0 & 0 & 0 & 0 \\ 0 & R_2 & 0 & 0 & 0 & 0 & 0 \\ 0 & 0 & R_1 & 0 & 0 & 0 & 0 \\ 0 & 0 & 0 & R_2 & 0 & 0 & 0 \\ 0 & 0 & 0 & 0 & R_1 & 0 & 0 \\ 0 & 0 & 0 & 0 & 0 & R_2 & 0 \\ 0 & 0 & 0 & 0 & 0 & 0 & R_3 \end{bmatrix}$$

$c_1 = \cos\theta$

$s_1 = \sin\theta$

$$[R_1] = \begin{bmatrix} c_1 & 0 & 0 & s_1 & 0 & 0 \\ 0 & c_1^2 & c_1 s_1 & 0 & c_1 s_1 & s_1^2 \\ 0 & -c_1 s_1 & c_1^2 & 0 & -s_1^2 & c_1 s_1 \\ s_1 & 0 & 0 & c_1 & 0 & 0 \\ 0 & -c_1 s_1 & -s_1^2 & 0 & c_1^2 & c_1 s_1 \\ 0 & s_1^2 & -c_1 s_1 & 0 & -s_1 c_1 & c_1^2 \end{bmatrix}$$

$$[R_2] = \begin{bmatrix} 1 & 0 & 0 & 0 & 0 & 0 \\ 0 & c_1 & s_1 & 0 & 0 & 0 \\ 0 & -s_1 & c_1 & 0 & 0 & 0 \\ 0 & 0 & 0 & c_1^2 & 2s_1c_1 & s_1^2 \\ 0 & 0 & 0 & -c_1s_1 & c_1^2-s_1^2 & s_1c_1 \\ 0 & 0 & 0 & s_1^2 & -2s_1c_1 & c_1^2 \end{bmatrix}$$

$$[R_3] = \begin{bmatrix} c_1 & s_1 \\ -s_1 & c_1 \end{bmatrix}$$

APPENDIX B

MATRIX $[a]$: See Fig. 4 for definition of various symbols.

Defining

$$b_i = y_j - y_m$$

$$c_i = x_m - x_j$$

$$d_i = x_j y_m - x_m y_j$$

$\triangle$ = area of triangle.

$$[a] = \begin{bmatrix} a_{11} & a_{12} & a_{13} & a_{14} & a_{15} & a_{16} \\ a_{21} & a_{22} & a_{23} & a_{24} & a_{25} & a_{26} \end{bmatrix}$$

$$a_{11} = (d_i + b_i \xi + c_i \eta)/2\triangle$$

$$a_{13} = (d_j + b_j \xi + c_j \eta)/2\triangle$$

$$a_{15} = (d_m + b_m \xi + c_m \eta)/2\triangle$$

$$a_{12} = a_{11} \qquad a_{14} = a_{13} \qquad a_{16} = a_{15}$$

$$a_{21} = a_{22} = a_{11} \qquad a_{23} = a_{24} = a_{13}$$

$$a_{25} = a_{26} = a_{15}$$

MATRIX [b]:

$$[b] = \frac{1}{2\Delta}\begin{bmatrix} b_i & 0 & b_j & 0 & b_m & 0 \\ 0 & c_i & 0 & c_j & 0 & c_m \\ c_i & b_i & c_j & b_j & c_m & b_m \end{bmatrix}$$

MATRIX [c]:

$$[c] = \frac{E}{(1-\nu^2)}\begin{bmatrix} 1 & \nu & 0 \\ \nu & 1 & 0 \\ 0 & 0 & \frac{(1-\nu)}{2} \end{bmatrix}$$

ROTATION MATRIX [R]:

$$[R] = \begin{bmatrix} R_1 & 0 & 0 \\ 0 & R_1 & 0 \\ 0 & 0 & R_1 \end{bmatrix}$$

$$[R_1] = \begin{bmatrix} r_{11} & r_{12} & r_{13} \\ r_{21} & r_{22} & r_{23} \\ r_{31} & r_{32} & r_{33} \end{bmatrix}$$

$$x_{ij} = x_i - x_j; \quad y_{ij} = y_i - y_j; \quad z_{ij} = z_i - z_j$$

$$L = \sqrt{(x_{ji}^2 + y_{ji}^2 + z_{ji}^2)}$$

$$P = \sqrt{(x_{mj}^2 + y_{mj}^2 + z_{mj}^2)}$$

$$r_{11} = x_{ji}/L \qquad r_{12} = y_{ji}/L \qquad r_{13} = z_{ji}/L$$

$$r_{21} = x_{mj}/P \qquad r_{31} = y_{mj}/P \qquad r_{32} = z_{mj}/P$$

$$r_{31} = r_{11}r_{23} - r_{13}r_{22}$$

$$r_{32} = r_{13}r_{21} - r_{11}r_{23}$$

$$r_{33} = r_{11}r_{22} - r_{12}r_{21}$$